DNA binding fluorescent proteins as single-molecule probes

Article *in* The Analyst · April 2020

DOI: 10.1039/D0AN00218F

4 authors:

Kyubong Jo
Sogang University
61 PUBLICATIONS **1,263** CITATIONS
SEE PROFILE

Xuelin Jin
6 PUBLICATIONS **34** CITATIONS
SEE PROFILE

Natalia Diyah Hapsari
Sogang University
3 PUBLICATIONS **12** CITATIONS
SEE PROFILE

Lee Seonghyun
Institute for Basic Science
27 PUBLICATIONS **314** CITATIONS
SEE PROFILE

Analyst

ROYAL SOCIETY OF CHEMISTRY

CRITICAL REVIEW

View Article Online
View Journal

Cite this: DOI: 10.1039/d0an00218f

DNA binding fluorescent proteins as single-molecule probes

Xuelin Jin,†[a] Natalia Diyah Hapsari,†[a,b] Seonghyun Lee[a] and Kyubong Jo *[a]

DNA binding fluorescent proteins are useful probes for a broad range of biological applications. Fluorescent protein (FP)-tagging allows DNA binding proteins expressed within a living cell to be directly visualised, in real-time, to study DNA binding patterns and dynamics. Moreover, FP-tagged DNA binding proteins (FP-DBP) have allowed the imaging of single proteins bound to large elongated DNA molecules with a fluorescence microscope. Although there are numerous DNA binding proteins, only a small portion of them have been exploited to construct FP-DBPs to study molecular motion in a cell or *in vitro* single-molecule visualisation. Therefore, it would be informative to review FP-DBP for further development. Here, we summarise the design of FP-DBPs and their brightness, photostability, pK_a, maturation rate, and binding affinity (K_d) characteristics. Then, we review the applications of FP-DBP in cells to study chromosome dynamics, DNA replication, transcription factors, DNA damage, and repair. Finally, we focus on single DNA molecule visualisation using FP-DBP.

Received 2nd February 2020,
Accepted 18th April 2020

DOI: 10.1039/d0an00218f

rsc.li/analyst

Introduction

The visualisation of DNA molecules in the cell nucleus has provided essential biochemical information on processes such as DNA replication, gene regulation, and DNA damage repair. Moreover, the visualisation of elongated DNA molecules within nano- and microfluidic devices has provided a platform to study biochemical reactions,[1] such as chemical modifications[2,3] and DNA damage at the single-molecule level.[4–7] Many studies have been conducted to monitor enzymatic motion and functions on a large elongated DNA molecule, such as the dynamics of DNA looping,[8] DNA replication forks,[9,10] the movement of DNA translocases,[11] and the role of polymerase subunits.[12] Since DNA molecules are spectrophotometrically silent, they must be stained with dyeing materials for microscopic observation. Therefore, the development of DNA staining materials has been essential to make progress in DNA research. The first stain was Giemsa dye, a mixture of methylene blue, eosin, and Azure B, developed in 1904, which is still a powerful tool in cytogenetic chromosome analysis.[13] Since the use of agarose gel electrophoresis began in 1967,[14] DNA staining became essential. In the beginning, radioactive labelling was the only way to stain DNA in a gel. From 1972, ethidium bromide became a primary staining reagent by intercalating with DNA after gel electrophoresis.[15] In 1975, Russell *et al.* developed 4′,6-diamidino-2-phenylindole (DAPI) to stain DNA by binding in the minor grooves of AT-rich sequences.[16] In 1992, Glazer *et al.* developed a high-contrast staining reagent for cyanine dimers such as thiol-orange homodimer (TOTO-1) and oxazole yellow homodimer (YOYO-1).[17,18] These dyes became the primary staining reagents to visualise single-molecule DNA on a microscope. In addition, membrane-permeable cyanine dyes or SYTO have been used to stain DNA in a viable cell.[19]

There has been a great effort to visualise specific sequences in DNA. A well-known method is fluorescence *in situ* hybridisation (FISH), developed in the early 1980s, which uses fluorescent probes that bind to complementary DNA sequences to determine the presence of specific DNA sequences in chromosomes.[20,21] FISH has been furthered developed into fibre FISH, developed in the early 1990s to increase resolution.[22,23] In 1993, Schwartz and his colleagues introduced Optical Mapping, which generated a sequence-specific barcode-like pattern by digesting elongated large DNA molecules using a restriction enzyme.[24,25] This pioneering work has led to the development of various approaches for sequence-specific labels on single DNA molecules, enzyme-based labelling like nick translation (Nanocoding),[26–28] methyltransferase-direct click chemistry (Fluorocode),[29,30] and affinity-based labelling like denaturation–renaturation (DR) mapping,[31] competitive binding assay,[32] and A/T specific pyrrole-polyamides.[33]

DNA binding peptide motifs and proteins are promising materials for labelling DNA molecules for both

[a]*Department of Chemistry and Interdisciplinary Program of Integrated Biotechnology, Sogang University, Seoul, 04107, Republic of Korea. E-mail: jokyubong@sogang.ac.kr*
[b]*Chemistry Education Program, Department of Mathematics and Science Education, Sanata Dharma University, Yogyakarta, 55282, Indonesia*
† These two authors equally contributed to this work.

homogeneous[34–37] and specific staining.[38,39] More importantly, there are numerous DNA binding proteins or peptide motifs available. Since the early 1990s, there have been attempts to visualise DNA–protein complexes using fluorescent dye-coupled antibodies.[40–43] Since then, fluorescent protein fused DNA binding proteins (FP-DBPs) have gradually replaced organic dyes for the visualising DNA and its associated biomolecules within cells.[44] The most notable feature is that FP-tagged proteins are usually expressed within the cells. This feature leverages genetic regulation that is not accessible using synthetic dyes or quantum dots.[45] Moreover, FP-DBPs can be readily loaded into the cell nucleus by simple gene construct designs using molecular biology tools.[46] Thousands of FPs with different colours and various properties are available.[47] FP-DBPs have additional advantages over organic dyes for DNA staining. Several prior studies have described the low cytotoxicity of FPs.[48,49] In contrast, organic fluorescent dyes are often cytotoxic.[50,51] Additionally, FP-DBPs do not cause photo-induced DNA breaks because their fluorophores are buried in β-barrels,[34] while intercalating organic fluorescent dyes cause photo-induced DNA breaks under continuous laser illumination.[52] Moreover, most FP-DBPs only minimally perturb the DNA structure,[34] which is a serious issue for intercalating organic fluorescent dyes.[53] Finally, FP-DBPs enable reversible DNA staining through pH shift or salt concentration changes, whereas it is almost impossible to reverse DNA staining for most organic staining reagents.[34] Consequently, the use of FP has revolutionised the fields of cell and molecular biology, because FP-tagging allows specific proteins to be directly and safely visualised, in real-time, to study their binding patterns and dynamics within a target organelle in a living cell.

In this review, we describe the development of DNA binding fluorescent proteins as probes both in cells and single-molecule experiments. We review how to design FP-DBP constructs and summarise their brightness, photostability, pK_a, maturation, and DNA binding affinity characteristics. Finally, we reviewed how FP-DBP has been utilised in analysing cells and visualising single DNA molecules.

Design of FP-DBPs

The design of an FP-DBP requires three elements: a DNA binding protein gene, a linker, and a fluorescent protein gene in a plasmid vector (Fig. 1). Most FP genes are commercially available or can be obtained through a non-profit plasmid repository, such as AddGene.[55] The FP gene can be placed at the N- or C- termini of the DBP gene, as shown in Fig. 1.[54] A linker between the FP and DBP genes is generally necessary. The linker has two to ten amino acid residues, typically consisting of serine and glycine, to enhance the solubility and flexibility of the linkers.[56] However, the C-terminus of GFP and related FPs have a floppy tail of ten amino acids, which often makes it unnecessary to insert an additional linker when fusing the C-terminus of FP and the N-terminus of the DNA binding protein.[57] The next step is to transform the expression

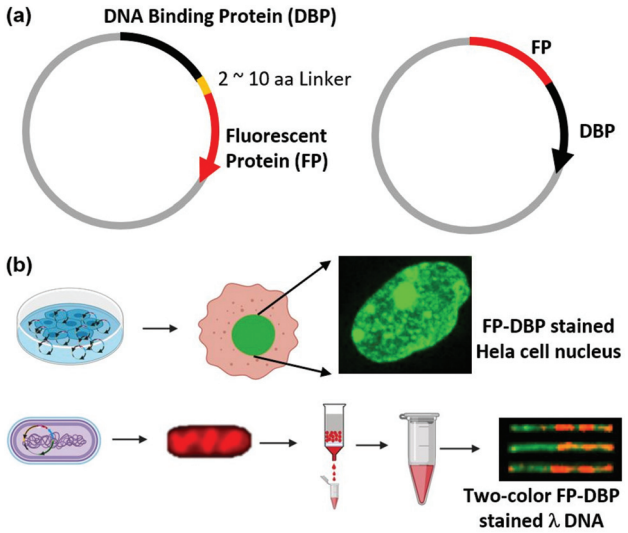

Fig. 1 Design of FP-DBPs. (a) Plasmid construct consisting of genes encoding a DNA binding protein, a linker, and a fluorescent protein, or the same elements in the opposite order.[54] The linker can be omitted if there is a floppy tail. (b) Illustration of how to apply FP-DBP to cells or perform *in vitro* experiments. For cell experiments, the expression of FP-DBP genes with a nuclear localisation sequence allows staining of DNA in thel nuclues. For DNA single-molecule observations, the plasmids are transformed into appropriate host cells followed by induction of FP-DBP expression, purification of FP-DBPs using affinity column chromatography, and observation of single DNA molecules stained with FP-DBPs. Reproduced from ref. 34 with permission from Oxford University Press, copyright 2015 [Creative Commons Attribution License (http://creativecommons.org/licenses/by/4.0/)]; reproduced from ref. 38 with permission from The Royal Society of Chemistry, copyright 2019 and made in ©BioRender – biorender.com.

vector into a host cell with or without an organelle targeting sequence. Obtaining purified FP-DBP protein requires protein purification steps, which typically consist of affinity chromatography and additional fast protein liquid chromatography (FPLC) steps.[34]

Problems are often encountered during the construction of the FP-DBP construct. Snapp summarised a troubleshooting guide (Table 1) for FP fused proteins in his review paper.[54] The first common issue is that FP does not fluoresce for several possible reasons. Many FPs do not fluoresce in low pH environments, which can be solved by using low pK_a FPs.[58] Improper folding of FP-fused proteins can result in a lack of fluorescence or malfunction, which requires inserting an appropriate linker between the FP and DBP to release steric hindrance.[59–61] Another issue is FP aggregation, primarily because of the constitutive expression of FP fused protein. As a solution, Ratz *et al.* reported a method of CRISPR/Cas9 genome editing to knock-in a gene into a cell's host genome to express FP-fused proteins at the endogenous level.[62] In addition, there are FPs starting with *m* representing monomer that tend not to aggregate. FP-fused proteins are often localised into an unexpected subcellular organelle. Recently, Palmer and Freeman systematically analysed this localisation issue in terms of N-terminal and C-terminal

Table 1 A troubleshooting guide for the design of FP-DBPs.[54]

Problem 1: FP-DBP is not fluorescent.	
Cause:	(1) Environmental condition (low pH) suppresses fluorescence. (2) FP-DBP is not folded appropriately. (3) FP-DBP is not expressed or is highly unstable.
Solution:	(1) Use fluorescent proteins which are tolerant of different environments. (2) Insert short linkers between FPs and DBPs. The linkers help to ensure appropriate folding of FPs and DBPs. (3) Perform immunoblot analysis or immunoprecipitation analysis to check if the FP-DBP is expressed.
Problem 2: FP-DBP is nonfunctional.	
Cause:	(1) FP agglomerates. (2) FP sterically hinder DBP folding or obstruct DBP functional domains.
Solution:	(1) Use monomeric fluorescent proteins (2) Avoid overexpression by CRISPR/Cas9-mediated genome editing strategies resulting in endogenous level expression (3) Insert short linkers between FPs and DBPs (4) Change the placement of FPs in fusion proteins.
Problem 3: FP-DBP does not localize correctly.	
Cause:	(1) FP interferes with DBP's targeting sequence. (2) FP oligomerizes.
Solution:	(1) Change the placement of fluorescent proteins in fusion proteins. (2) Insert short liners between FPs and DBPs. (3) Use monomeric FPs.

linked FP fused proteins.[63] They are categorised into three groups. Group 1: both are the same as reverse transfection; group 2: different locations depending on whether they are N-terminal or C-terminal; group 3: C-terminal fusing results in expected localisation but there is no localisation for the N-terminal fusion.

Characteristics of FP-DBP

The essential characteristics of FP-DBPs need to be determined. These include brightness, pK_a, maturation time, and DNA binding affinity. Brightness depends on the FP constituent, while DNA binding affinity depends on the DBP constituent. To obtain the information concerning FP characteristics, FPbase.org is a useful database characterising 771+ FPs.[47] This website is a free, open-source, and community-editable database, and the number of FPs included keeps increasing. It provides information on FP structure, sequence, evolutionary origin, photostability, brightness, pK_a, maturation, lifetime, references, and an AddGene link. Furthermore, Google search usually includes results from FPbase as one of the top lists. Therefore, FPbase is quite useful for finding FP characteristics and references. In particular, the protein table in FPbase provides useful information that can be sorted by an attribute. Here, we select dozens of FPs to analyse and compare their characteristics from the FPbase protein table. The Fluorophores.org (fluorophores.tugraz.at) community-editable database is available for organic fluorescent dyes. This website also provides information regarding the chemical structure, quantum yield, excitation, and emission spectra of fluorophores, as well as commercial sellers and their websites. However, more data need to be added to this database as there is a lack of information about many fluorophores. Moreover, the data do not comprise extinction coefficient values, which are essential to calculate brightness.

Brightness: extinction coefficient × quantum yield

Brightness is the most important FP characteristic because it determines the detection sensitivity as well as the signal-to-noise ratio. In general, the brightness of a fluorophore is defined as the product of the extinction coefficient and the quantum yield ($b = \varepsilon \times \phi$).[64] EGFP and mCherry are the most popular FPs, but there are many other brighter FPs. There has been an effort to improve FP brightness by mutagenesis.[65,66] According to the FPbase protein table, AausFP1 is the brightest, b = 164.9, discovered to date, with a nearly perfect quantum yield (φ = 0.97) and a peak extinction coefficient of ε = 170 mM^{-1} cm^{-1}, making it nearly five-fold brighter than EGFP on a per-molecule basis.[67] Among red-colour FPs, RRvT is the brightest (b = 117.92). It was developed from tdTomato (b = 95.2) by ten iterative rounds of directed protein evolution.[68] The dimeric nature of RRvT explains its high brightness. Fig. 2 compares FPs with common organic fluorescent dyes, including DNA-bound YOYO-1 and TOTO-1. It is notable that RRvT and AausFP1 developed by direct evolution are

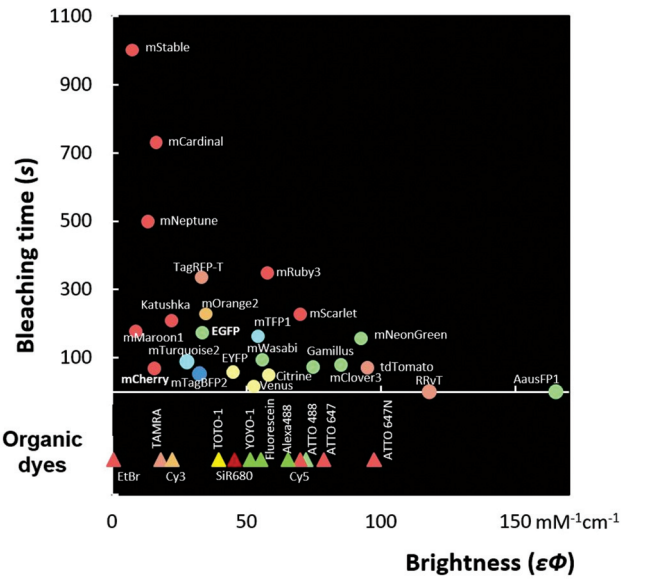

Fig. 2 FP brightness and photostability compared with organic dyes: The colours represent the emission of FPs (circles) and organic dyes (triangle). The bleaching time represents photostability and the brightness is the product of extinction coefficient (ε) and quantum yield (φ) of the particular fluorophore. FPs: mStable,[69] mCardinal,[70] Katushka,[71] TagRFP-T,[72] mRuby3,[73] mOrange2,[72] mScarlet,[74] mMaroon1,[75] mNeptune,[76] EGFP,[73] mNeonGreen,[77] mTFP1,[78] mWasabi,[79] mTurquoise2,[80] Gamillus,[81] mClover3,[73] tdTomato,[82] mCherry,[82] mTagBFP2,[83] EYFP,[84,85] Citrine,[86] Venus,[87] RRvT,[68] AausFP1.[67] Organic dyes: EtBr,[88] TAMRA,[89] Cy3,[89] TOTO-1, SiR 680, YOYO-1,[88] Fluorescein,[89] Cy5,[89,90] ATTO 488,[89] Alexa 647,[89] and ATTO 647N.[89,90]

markedly brighter, even compared with the brightest organic dye (ATTO647N).

Brighter FPs are more useful than less bright FPs or organic fluorescent dyes in various applications because they require a comparatively smaller dose of excitation light, which may reduce phototoxicity for cells expressing fluorescent proteins.[91,92] In addition, they are effective for low copy proteins expressed in a cell.[93–95] For example, Glauser *et al.* compared mNeonGreen (b = 92.8) and EGFP (b = 33.6) reporters in *C. elegans*.[93] They show similar patterns, but low expression copies were detected with mNeonGreen but not EGFP reporters.

The y-axis in Fig. 2 shows FP bleaching time ($\tau_{1/2}$), which is a critical factor for long-time observation. The FPbase.org database includes a caution in interpretation of the findings, given that bleaching times are dependent on the intensity of light source. Many of the measurements are made using a widefield microscope with an arc lamp. For example the bleaching time of EGFP is 174 s (Fig. 2), while the use of a 1.5 mW laser has produced a time of 50.1 s.[96] To date, no studies have reported the bleaching times for AausFP1 and RRvT (the brightest FPs); thus, their values are set to zero. The longest bleaching time is 1002 s for mStable.[69] The shortest is 15 s for Venus.[87] In addition to Venus, two other yellow colours are relatively unstable, such as EYFP (60 s)[84,85] and Citrine (49 s).[86] For green colours, EGFP (174 s)[73] and mNeonGreen (158 s)[77] are relatively stable. For red colours, mCherry (68 s)[82] is not stable. However, there are long bleaching time red colour FPs, such as mStable (1002 s),[69] mCardinal (730 s),[70] and Katushka (700 s).[71] Among the red colours, mRuby3 (349 s, b = 57.6) and mScarlet (227 s, b = 70) have long bleaching times with high brightness. Accordingly, Fig. 2 can be used as a guideline to choose the best FP for a given application.

pK_a & maturation time

Fig. 3a shows the pK_a values for FPs ranged from 2.5 for mBlueberry2[97] to 8.6 for Kohinoor.[100] FP's pK_a is important because fluorescence is half of the maximum when pK_a equals the pH.[106] FPs are usually brightest at pH 8–9.[107,108] If pH is higher than 10, FPs lose their fluorescence.[109,110] If the pH is lower than their pK_a, the FP's fluorescence decreases to less than half of its maximum brightness. The EGFP pK_a = 6.0,[73] and the mCherry pK_a = 4.5.[82] There are low pKa FPs, such as mBlueberry2 (pK_a = 2.5),[97] mTagBFP (pK_a = 2.7),[72] mTurquoise2 (pK_a = 3.1),[80] and Gamilus (pK_a = 3.4)[81] developed for low pH subcellular organelles like vacuoles (pH = 5.2), secretory vesicles (pH = 5.0–6.0), and lysosomes (pH < 5.5).[111] However, pK_a is not critical for constructing FP-DBPs because DNA molecules are primarily located only in the nucleus (pH 7.2–7.3) or mitochondria (pH 7.9–8.1).

Fig. 3b shows the maturation time of various FPs during expression in a cell. FP requires time for folding and subsequent chemical maturation of the fluorophores. Fluorophore maturation rates vary from 1.8 min (mAmeritrin)[105] to days (Slow-FT: 69 h).[101] EGFP has a 14.5 min,[104] and mCherry has a 43.4 min[104] maturation time. FP tagging of short-lived proteins should use FPs with a rapid maturation rate.[112] Many applications require a consideration of balanced timing for the maturation of FPs and DBPs. For example, a DNA strand can lose its function during the slow process of FP folding.

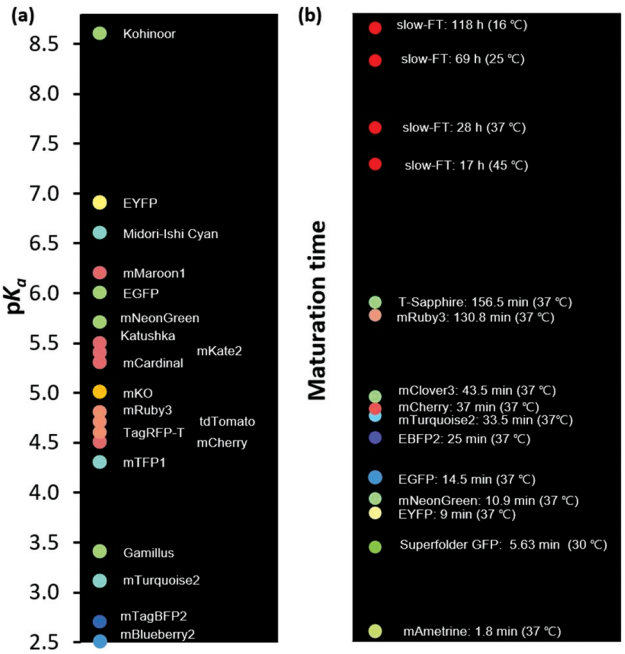

Fig. 3 FP's pK_a and maturation time (a) pK_a values of 19 FPs. Kohinoor,[97] EYFP,[84,85] Midori-Ishi Cyan,[98] mMaroon1,[75] EGFP,[73] mNeonGreen,[77] Katushka,[71] mKate2,[99] mCardinal,[70] mKO,[98] mRuby3,[73] tdTomato,[82] TagRFP-T,[72] mCherry,[82] mTFP1,[78] Gamillus,[81] mTurquoise2,[80] mTagBFP2,[83] mBluberry2.[100] (b) Maturation times of 15 FPs at a given temperature. The y-axis is the log-scale in min. Slow-FT,[101] EBFP2,[102] Superfolder GFP,[103] mTurquoise2,[104] T-Sapphire,[104] EGFP,[104] EYFP,[104] mNeonGreen,[104] mClover3,[104] mCherry,[104] mRuby3,[104] mAmetrine.[105] Each colour represents the emission wavelength of each FP.

DNA binding affinity of FP-DBP

DNA binding capability is a key component in the characterisation of FP-DBPs. DNA binding affinity is generally measured by the dissociation constant (K_d). More specifically, $1/K_d$ represents the binding affinity for target DNA. There are several methods to measure this value, such as EMSA, ELISA, equilibrium dialysis, SPR, analytical ultracentrifugation, spectroscopic assays, and isothermal titration calorimetry.[113–120]

It is notable that FP-tagging changes binding affinity as does its position. For example, Fig. 4 shows that whether the FP is N- or C- terminal affects the affinities of FP-DBPs, even when the FP and DBPs are the same.[121,122] RHAU53-CFP has a higher binding affinity than CFP-RHAU53. The addition of a linker also affects DBP binding affinity. Therefore, it is not trivial to apply the known affinity of DNA binding proteins to newly constructed FP-DBPs. It is necessary to measure the binding affinity of newly made FP-DBPs after purification.

Table 2 lists FP-DBP applications and K_d values from 90 previously published studies. Most applications reported are cell-

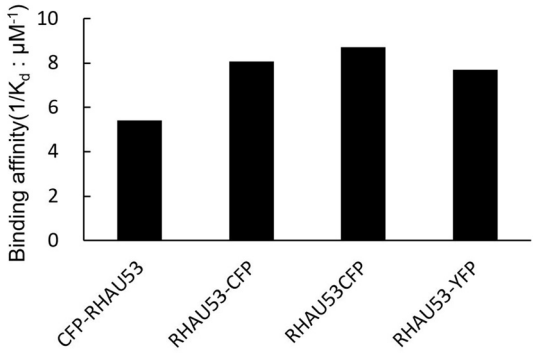

Fig. 4 The affinity of FP-DBPs for DNA depending on FP positions. CFP-RHAU53, RHAU53-CFP, RHAU53CFP without a linker, and RHAU140-CFP,[121] RHAU53-YFP.[122] A hyphen represents a linker.

based. Twenty studies reported K_d values through protein purification and *in vitro* assays. The data reveal variation in K_d from 0.1 nM to 1 mM, with most values in the nanomolar range, suggesting high binding affinity of FP-DBPs for DNA binding proteins. Moreover, it is necessary to consider that the affinity of FP-DBPs can differ depending on target or random sequences.

Applications of FP-DBPs in cells

Table 2 lists FP-tagged DNA binding proteins that have been applied to study cell biology. From this table, this section categorizes them into chromosomal dynamics, DNA replication, transcription factors, and DNA damage and repair. This section will discuss further examples.

FP-DBP visualisation of mitotic chromosome dynamics

Fig. 5a shows mitotic errors resulting in the formation of micronuclei during the RPE-1 cell division.[213] Micronuclei is a common nuclear aberration leading to chromothripsis, a fatal mutational process commonly observed in cancers.[215–217] CENPA-GFP and Centrin 1-GFP enable to detect the micronuclei during cell mitosis. In this study, CLEM, a combination of fluorescence microscopy and electron microscopy, also detected the defects in nuclear envelope assembly for micronuclei at later stages of cytokinetic furrowing. At later stages of cytokinetic furrowing, the nuclear pore complexes are present on the nuclear envelope of the primary nucleus, but not on the nuclear envelope of the micronucleus. This irreversible nuclear envelop assembly defect results in chromothripsis.

Fig. 5b illustrates telomere aggregation during mitosis using YFP-TRF1 (telomeric repeat-binding factor 1).[127] Telomeres are short non-coding DNA repeats at the ends of linear chromosomes.[218] TRF1 is a subunit of shelterin, a six-subunit protein complex (TRF1, TRF2, POT1, TPP1, TIN2, and Rap1) that allows cells to distinguish the natural ends of chromosomes from sites of DNA damage.[219] TRF1 binds to tel-

Table 2 FP-DBP applications and K_d

Application	DBP	K_d (nM)	FP-DBP	Ref.
Chromosome dynamics	CENP-S		mCherry-CENP-S, CENP-S-mCherry, CENP-S-EGFP, EGFP-CENP-S, EGFP-CENP-X, CENP-X-mCherry, mCherry-CENP-T	123
	CENP-X		CENP-T-mCherry	
	CENP-T		EGFP-CENP-T	
	Cse4		Cse4-GFP	124
	CENP-A		ECFP–EYFP–CENP-A EGFP–CENP-B	125
	CENP-B		CENP-B–EYFP	
	CENP-B		CENPB-GFP	126
	TRF1		YFP-TRF1	127
DNA replication	DnaA	0.9	YFP-DnaA	128, 129
	DnaX		DnaX-mCherry	
	SeqA		SeqA–PAmCherry	130
	RFA1		RFA1-EGFP	131
	RFA2		RFA2-EGFP	
	RFA3		RFA3-EGFP	
	HOXC13	56	GFP-HOXC13 mCherry-HOXC13	132–134
DNA transcription	FgHltf1		FgHltf1-GFP	135
	AcMybA		AcMybA-RFP	136
	CRC		GFP-CRC	137
	RUNX2		RUNX2-GFP	138
	FMBP-1		EGFP-FMBP-1	139
	HIF-1 α		HIF-1 α -EGFP	140
	HIF-2 α		EGFP-HIF-2α	
	AtSTKL1		GFP-AtSTKL1	141
	Scr		mCitrine-Scr	142
	RFX1	153	RFX1-GFP	143, 144
	HapX	2.54	HapX-VENUS	145, 146
	VIP1		VIP1-GFP	147
	GalR	4	GalR-Venus	148, 149
	Oct4	25	GFP-Oct4	150
	Sox2	24	mRFP-Sox2	150, 151
	AtMYBL		GFP-AtMYBL	152
	PAX5	5	YFP-PAX5-PML	153, 154
	LexA	0.1	LexA-GFP	155, 156
	SclR		SclR-EGFP	157
	LXRα		CFP-LXRα	158
	LXRβ		CFP-LXRβ	
	Fep1		Fep1-GFP	159
	TabZIP1		TabZIP1-GFP	160
	CrzA		CrzA-GFP	161
	C/EBP		GFP-C/EBP	162
	OsLG1		OsLG1-RFP	163
	OsWRKY53		sGFP-OsWRKY53	164
	FoxI1		FoxI1-GFP	165
	MTF-1		EGFP-MTF-1	166
	WT1	0.5	GFP-WT1	167, 168
	PU.1		GFP-PU.1	169
	Snail		GST-Snail-GFP	170
	IE1		IE1-GFP	171
	FOXO1	93	FOXO1-GFP	172, 173
	Pit-1		GFP-Pit-1	174
	TTF2		GFP-GST-TTF2	175
	PacC		PacC-GFP	176
	ARNT	10.4	GFP-ARNT	177, 178
	Terra		GFP-Terra	179
	ABF-1		GFP-ABF-1	180
	Pip		GFP-Pip	181
	p65	1060	GFP-p65	182, 183
	FBP		GFP-FBP	184, 185
	PDX-1		PDX-1-GFP	186
	Stat5B		GFP-Stat5B	187
	IRF-1		IRF-1−GFP	188
	LEF-1	1	GFP–LEF-1	189, 190
	TBP	16	GFP-TBP	191, 192

Table 2 *(Contd.)*

Application	DBP	K_d (nM)	FP-DBP	Ref.
DNA damage and repair	Rad51	170	Rad51-GFP	193–195
	Rad52	6	Rad52-RFP	
	Ddc2		Ddc2-GFP	
	RecA	210	RecA-GFP	196, 197
	N protein		N-GFP	198
	53BP1		53BP1-GFP	199–201
	Ku80		EGFP-Ku80	202
	Dpb11		Dpb11-YFP	203
	Gam		Gam-GFP	204
	AddA		AddA-GFP	205
	XRCC4		YFP-XRCC4	206, 207
			CFP-XRCC4	
	Ligase IV	160	YFP-LigaseIV	206, 207
	XPA	68.7	XPG-EGFP	208, 209
	PCNA		EGFP-XPA	
			EGFP-PCNA	
	PC4		GFP-PC4	210
	DDB1		mCherry-DDB1	211
	DDB2		eYFP-DDB2	
	p21		p21-GFP	212

omeres as a dimer throughout cell division.[220–222] YFP-TRF1 visualised chromatin bridges are indicated by white arrows between the chromosomes of daughter cells that do not disappear during any part of mitosis. They used H2B-RFP (H2B: histone component) as a control to show other parts of DNA during the mitosis.

Fig. 5c shows chromosomal segregation in mycobacteria (*M. smegmatis*) using EGFP-ParA and ParB-mCherry.[214] Bacterial chromosome segregation requires ParA and ParB proteins.[223] ParA, a Walker A ATPase, interacts with DNA nonspecifically.[224] ParB, a DNA-binding protein, binds to parS sequences, usually located in proximity to the oriC, thereby forming segrosomes, the nucleoprotein complexes. After DNA replication, there is only one ParB-mCherry focus close to the old pole (Po), and GFP-ParA accumulates at the new pole (Pn). The time-lapse images illustrate the dynamic localisation of ParA and ParB, each of which represents DNA and oriC sites. The extension of ParA fluorescence from the new cell pole towards the newly duplicated ParB complexes might be associated with the movement of one of the ParB complexes towards the new cell pole. The spatiotemporal localisation of proteins related to chromosome segregation explains the dynamic division of the mycobacterial chromosome as the schematic suggests (Fig. 5c).

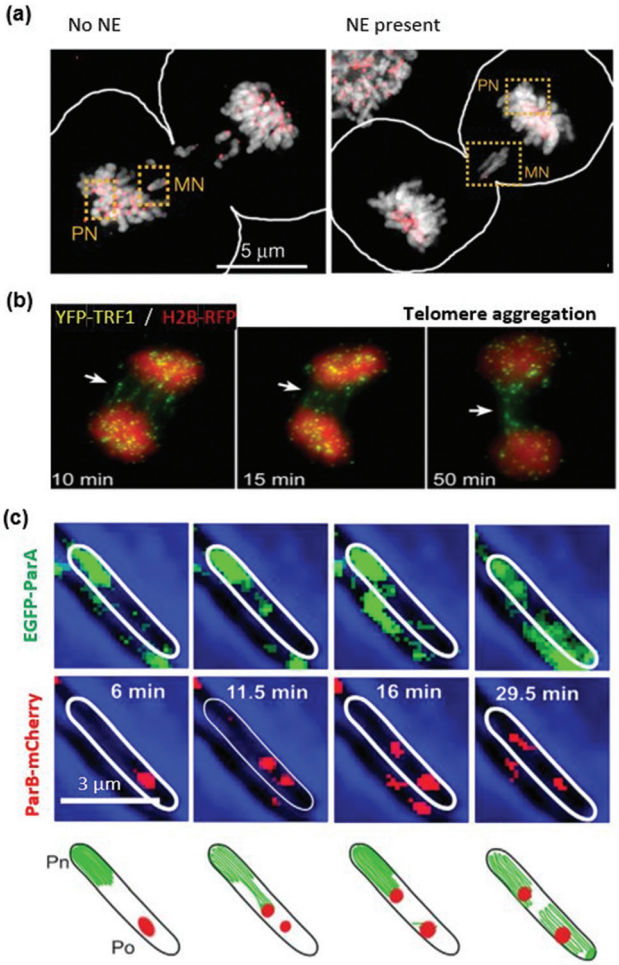

Fig. 5 FP visualisation of chromosome dynamics. (a) Correlative light-electron microscopy (CLEM) images of mitotic errors. Left: RPE-1 cells at an earlier stage of the cytokinetic furrowing. Right: a later stage of the cytokinetic furrowing. At later stages, nuclear envelopes (NE) are present at both primary nuclei (PN) and micronuclei (MN); on the other hand, there is no NE observed during the earlier stages. Grey: DNA. Red: kinetochores (CENPA-GFP) and centrosomes (Centrin 1-GFP). Scale: 5 μm. Reproduced from ref. 213 with permission from Springer Nature, copyright 2018. (b) Time-lapse observation of mouse embryonic stem cells expressing high levels of YFP–TRF1 and H2B–RFP. Formation of TRF1 bridges between segregating chromosomes. Reproduced from ref. 127 with permission from The American Society for Cell Biology, copyright 2014. (c) Localisation of GFP–ParA and ParB–mCherry during the cell cycle of M. smegmatis cells. Reproduced from ref. 214 with permission from John Wiley & Sons Ltd, copyright 2017. Time-lapse observation of ParB segregation using EGFP-ParA and ParB-mCherry. Schematic for mitotic separation process.

FP-DBP visualising DNA replication

Fig. 6 demonstrates three examples of the use of FP-DBP for visualising the DNA replication process. DNA replication is a key event in the cycle of all living cells. Fig. 6a illustrates where replication components exist during replication. They used LacI-CFP to visualise oriC. YFP-DnaA was used to visualise the replication initiation complex because DnaA is known to play an essential role in the regulation of replication initiation in bacteria by opening AT-rich strands.[225,226] The 20 min image shows that YFP-DnaA colocalizes with oriC to initiate DNA replication.[128] The 140 min image shows two separate oriC sites with YFP-DnaA in the middle. The right-most image used DnaX-mCherry to visualise the replication machinery, and YFP-YabA as a regulator to inhibit re-initiation during bacterial replication.[128] The localisation and intensity of the FP-DBP foci illustrate the DNA replication process.

Fig. 6b demonstrates the use of super-resolution imaging (PALM: photoactivated localisation microscopy) of

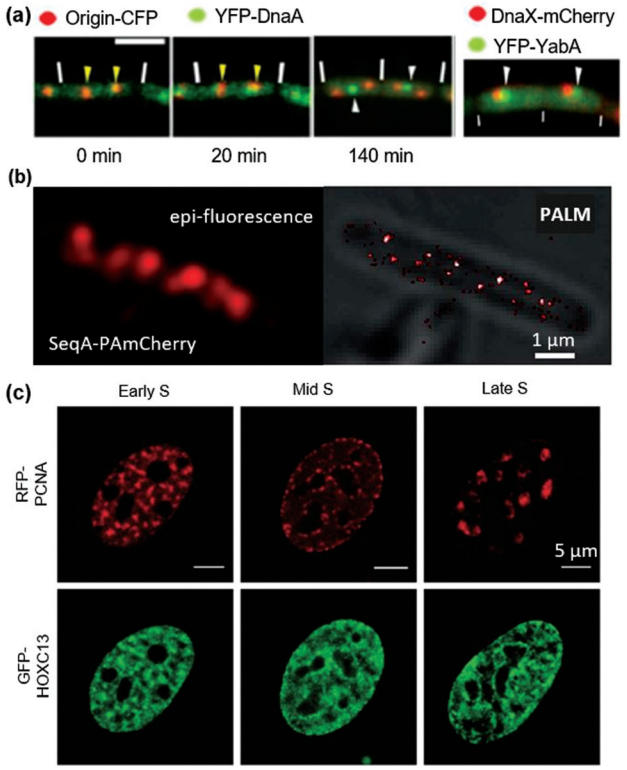

Fig. 6 FP visualisation of DNA replication. (a) Localisation of YFP-DnaA, oriC (LacI-CFP), replication machinery (DnaX-mCherry), and the re-initiation inhibitor (YFP-YabA). Reproduced from ref. 128 with permission from PLOS, copyright 2017 [Creative Commons Attribution License (http://creativecommons.org/licenses/by/4.0/)]. Scale bar: 2 μm. (b) PALM images of *E. coli* overexpressing SeqA-PAmCherry. Heterogeneous localisation of SeqA-PAmCherry. Reproduced from ref. 130 with permission from The Royal Society of Chemistry, copyright 2015. (c) NIH3T3 co-transfected with EGFP-HOXC13 and RFP-PCNA and three different patterns of replication foci: early S, mid S, and late S replication foci. Reproduced from ref. 132 with permission from Oxford University Press, copyright 2010.

SeqA-PAmCherry.[130] SeqA is a DNA binding protein regulating the initiation of DNA replication in *E. coli*.[227] In *E. coli*, newly replicated GATC sites are hemimethylated.[228] SeqA binds to hemimethylated GATC sites in newly replicated DNA, thereby preventing replication initiation by DnaA.[229] The *epi*-fluorescence image suggests their binding through the genome, but a super-resolution (PALM) image shows scattered hemimethylated regions (SeqA-PAmCherry) throughout the *E. coli* genome. Therefore, super-resolution microscopy improved the understanding of small-sized bacterial subcellular events.

Fig. 6c shows the location of DNA replication machinery and gene regulators in the eukaryotic nucleus. RFP-PCNA, a sliding clamp, represents DNA replication machinery, and GFP-HOXC13 is a homeotic regulator during the S phase.[132] The distribution of homeotic regulators (GFP-HOXC13) is similar to the distribution pattern of the early replicating machineries (RFP-PCNA) in the early S phase. However, they start diverging during mid-S phase, and finally, they completely separate in the late S phase.

FP-linked transcription factors

Fig. 7 illustrates the detection of FP-fused transcription factors. Transcription factors have the capability of binding to specific DNA sequences to regulate gene expression. In their early pioneering research in 1998, Patterson *et al.* utilised GFP-TBP (TATA-binding protein) in mitotic yeast cells (Fig. 7a).[192] Fig. 7b illustrates FoxI1-GFP (forkhead transcription factor) bound to chromosomes during mitosis.[165] In most cases, transcription factors are detached from condensed chromatin in mitosis.[230] However, FoxI1 is the first protein found to be bound to condensed chromatins during mitosis. The DAPI image also confirms the binding of Fox1-GFP to DNA. Fig. 7c illustrates an example of CrzA-GFP accumulation in nuclei before and after the addition of Ca^{2+}. CrzA is a zinc finger transcription factor in *Aspergillus nidulans*.[161] Active nuclear import and export machinery transports CrzA depending on cytosolic Ca^{2+} concentration. CrzA-GFP reveals the cellular response mechanisms in real-time by visualising the response to Ca^{2+} concentration changes. Fig. 7d shows an example of TabZIP1-GFP localisation to the nucleus of wheat leave cells infected with *Puccinia striiformis*.[160] TabZIP1 is a leucine zipper gene, isolated from wheat leaves infected by *Puccinia striiformis*. Fig. 7e shows an example of FgHLTF1-GFP,

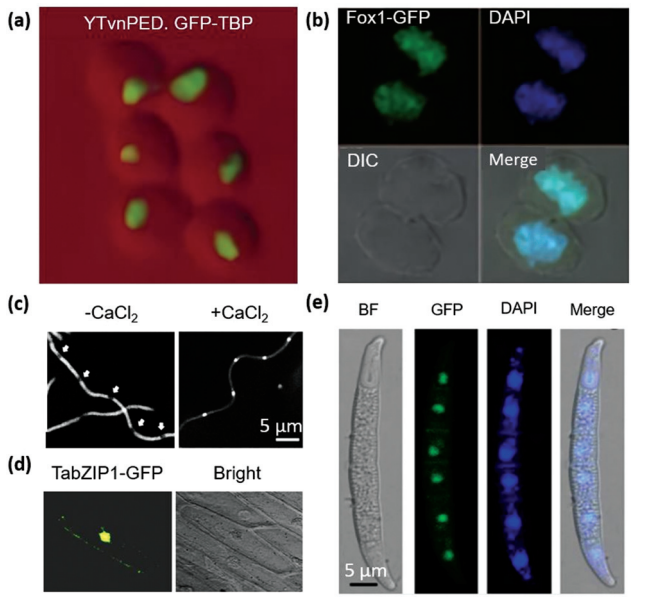

Fig. 7 FP linked transcription factors (a) GFP-TATA binding protein in yeast cells. Reproduced from ref. 192 with permission from John Wiley & Sons Ltd, copyright 1998. (b) FoxI1-GFP bound to mitotic chromatin during metaphase and telophase. Counterstaining cells expressing FoxI1-GFP with DAPI. Reproduced from ref. 165 with permission from American Society for Microbiology, copyright 2006. (c) Subcellular localisation of CrzA-GFP in MAD2055 cultured in fresh medium with or without 10 mM $CaCl_2$. Reproduced from ref. 161 with permission from Portland Press, copyright 2008. (d) Subcellular distribution of TabZIP1-GFP in onion epidermal cells. Reproduced from ref. 160 with permission from Elsevier Ltd, copyright 2009. (e) Localisation of FgHltf1-GFP in the conidia of *F. graminearum*. Reproduced from ref. 135 with permission from Springer Nature Limited, copyright 2019.

a histone-like transcription factor, localised in *Fusarium graminearum* nuclei.[135]

FP-DBPs are useful in the study of transcription factors by visualising transcription factor localisation and protein–DNA interactions in real-time response to changes in environmental conditions or transcription events.

FP-DBP visualisation of DNA damage and repair processes

Fig. 8 shows studies visualising DNA damage or its related phenomena with fluorescent proteins fused to DNA damage repair proteins. The accumulation of DNA damage recruits proteins to synthesise a repair complex at the damaged lesions. Fig. 8a shows the aggregation of p53-binding protein 1 (53BP1), a DNA damage response protein that plays important roles in choosing between the homologous recombination (HR) and non-homologous end-joining (NHEJ) repair pathways. Time-lapse images show the increased number of 53BP1-GFP foci in human breast cancer cells after UV-C irradiation.[200] In Fig. 8b, mCherry-53BP1 accumulates at laser micro-irradiated sites shown as a red line in the cells. Continuous expression of 53BP1 results in a rapid accumulation of 53BP1 at ionising radiation-induced foci.[231,232]

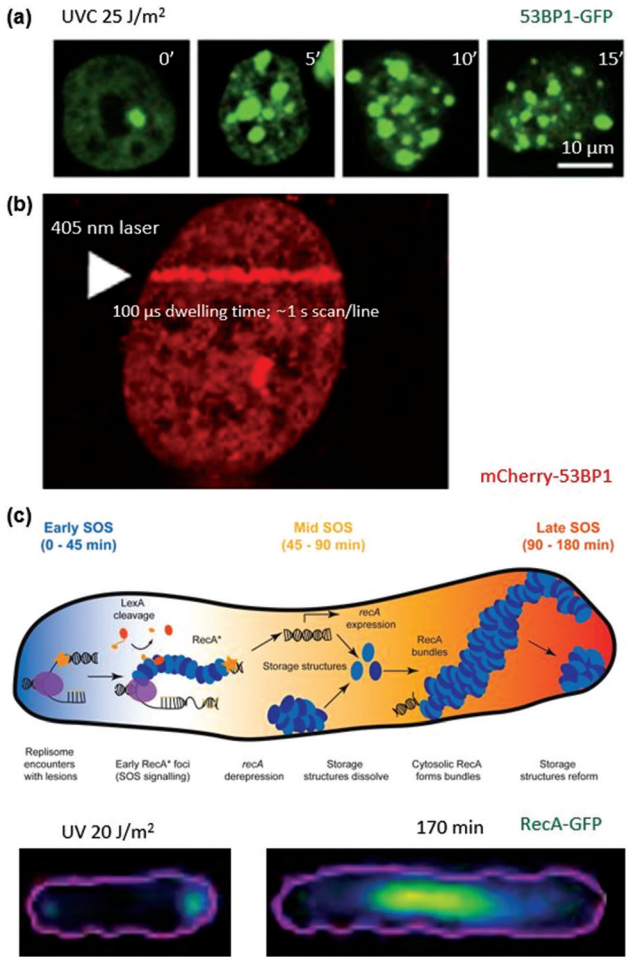

Fig. 8 FP visualising DNA damage and repair. (a) Formation of 53BP1-GFP foci in breast cancer cells after UVC irradiation. Reproduced from ref. 200 with permission from The International Institute of Anticancer Research, copyright 2016. (b) Accumulation of mCherry-53BP1 at DNA damage sites after laser-microirradiation. Reproduced from ref. 199 with permission from Oxford University Press, copyright 2019. (c) Schematic of the bacterial SOS response under UV exposure (20 J m^{-2}) and microscopic images of bacterial cells with RecA-GFP. The left image: after UV exposure and the right image: 170 min later. Reproduced from ref. 197 with permission from eLife Science Pblication, copyright 2019 [Creative Commons CC0 public domain dedication (https://creativecommons.org/publicdomain/zero/1.0/)].

Fig. 8c shows the SOS response after UV radiation in a bacterial cell. The SOS response regulates the synthesis of factors protecting and repairing the genome. In the SOS response, RecA forms filaments, which catalyse the autoproteolysis of LexA, a transcriptional repressor, to induce the expression of SOS genes.[233] DNA damage results in upregulated transcription of RecA.[234] As shown in Fig. 8c, after UV irradiation, RecA-GFP forms two foci in the ends of the bacterial cell.[197] After completion of DNA repair (170 min image), RecA-GFP accumulates in its bundle storage structures, shown as bright and large cigar-shaped regions in the fluorescent image.[197] These images support the schematic illustration of the SOS response.

FP-DBP based detection methods

The previous section described the use of FP-DBPs to monitor biochemical events to show the primary functions of DBPs. In contrast, FP-DBPs can be a tool to develop FP-DBP-based methods to detect other cellular changes unrelated to the native functions of DBPs. This section provides those examples of FP-DBP-based detection methods for double-strand DNA breaks, apoptosis, cell differentiation, and DNA methylation.

Fig. 9a presents FP-DBP-based methods for detecting double-strand DNA breaks using EGFP-MDC1, GamGFP, and N-GFP.[204,235] For example, EGFP-MDC1 detects γ-H2AX, a phosphorylated form of H2AX histones, and therefore, it can detect DNA double-strand breaks caused by several reasons that include reactive oxygen species. The method was developed to assess hazardous contaminants in river water. The second example is GamGFP and N-GFP, which label double-strand breaks in *E. coli*. However, the detection efficiency of GamGFP for dDNA damage is approximately 70%, while that of N-GFP is 12 to 18%.[204]

Fig. 9b illustrates the use of FP-DBPs to visualise cell apoptosis.[236] In this study, the cytoplasm of prostate cancer cells was stained using RFP and DNA in the cell nuclei was stained using H2B-GFP. The method enabled monitoring of cell destruction based on apoptosis, which continued for over 96 h.

Fig. 9c illustrates the detection of endoreduplication (replication of the nuclear genome in the absence of mitosis) using a photoconvertible FP-DBP (H2B-mEosFP) in the hypocotyl cells of *Arabidopsis*.[237,238] In this figure, mEosFP was converted using violet blue light and the plant was placed in the dark for 16 h. Next, nuclei of hypocotyl cells displayed a colour shift

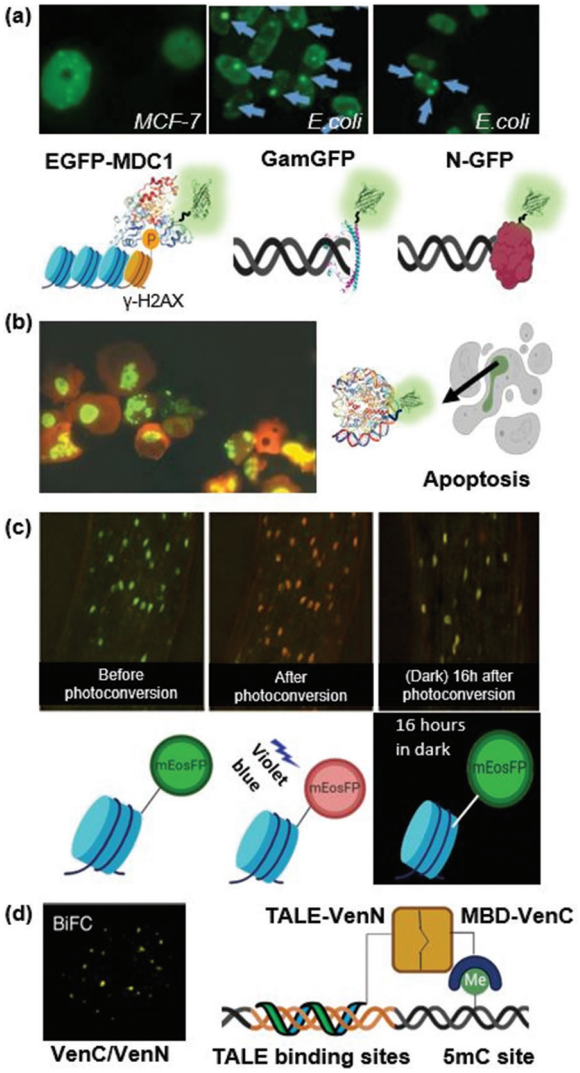

Fig. 9 FP-DBP-based detection method. (a) Detection of double-strand breaks with EGFP-MDC1,[235] GamGFP and N-GFP.[204] MDC1 (PDB 2ETX), Gam,[240] and EGFP (PDB 2Y0G). Reproduced from ref. 204 with permission from eLife Science Publications Ltd, copyright 2013 [Creative Commons Attribution License (https://creativecommons.org/licenses/by/3.0/)]; reproduced from ref. 235 with permission from Elsevier Ltd, copyright 2019; reproduced from ref. 240 with permission from National Academy of Sciences, copyright 2018. (b) Detection of apoptosis. Prostate cancer cells undergo apoptosis under exposure to paclitaxel. H2B-GFP enable staining of DNA in apoptotic cells.[236] Three-dimensional structure of the nucleosome (PDB 3AFA). Reproduced from ref. 236 with permission from The International Institute of Anticancer Research, copyright 2015. (c) Detection of cell endoreduplication. Arabidopsis hypocotyl cells expressing green H2B-mEosFP. After irradiation of violet-blue using six intervals of 45 s, photoconversion of green H2B-mEosFP to red occurs. After 16 h in darkness, the red color of the nuclei changes to green due to the increase of fresh H2B-mEosFP, which indicates endoreduplication.[238] Reproduced from ref. 238 with permission from The American Society of Plant Biologists, copyright 2012. (d) Bimolecular anchor sensor to detect DNA methylation. BiFC: bimolecular fluorescence complementation. BiAD sensor comprised MBD-VenC and TALE-VenN to detect 5mC sites in HEK293 cells.[239] Reproduced from ref. 239 with permission from Springer Nature Limited, copyright 2017 [Creative Commons Attribution 4.0 International License (http://creativecommons.org/licenses/by/4.0/)]. Illustrations prepared in ©BioRender – biorender.com.

from red fluorescence to green fluorescence, indicating an increase in fresh H2B-mEosFP content in the nuclei of cells undergoing endoreduplication. Cell enlargement was also evident.

Fig. 9d demonstrates a bimolecular anchor detector (BiAD) sensor to detect DNA methylation (5mC) with high specificity.[239] Bimolecular fluorescence complementation (BiFC) is a technology based on the association of fluorescent protein fragments. Venus can be divided into non-fluorescent C-terminal and N-terminal fragments, which are connected to methyl binding domain (MBD) and sequence-specific DNA binding protein (TALE: transcritipion activiator-like element), respectively. MBD-VenC and TALE-VenN bind to 5mC and TALE binding sites in HEK 293 cells. The VenC and VenN fragments then reconstitute fluorescent monomeric Venus proteins.

FP-DBP visualisation of single DNA molecules

So far, we have reviewed FP-DBP applications in cell images. However, DNA in a cell is compact, and it is difficult to analyse FP-DBP in the context of DNA genomic maps. Therefore, it is essential to unravel DNA molecule from a tangled coil.[241–243] Elongated DNA molecules are useful for various biochemical analyses in the context of the genomic map. Fig. 10 illustrates FP-DBP as a staining reagent for elongated large DNA molecules that we have developed since 2016.[34,36,244] This staining method is simple and straightforward with several distinct advantages. As shown in Fig. 10b, FP-DBP stained DNA is comparable with YOYO-1 stained DNA, in which stained DNA molecules were immobilised on a positively charged surface through microfluidic channels. However, as an intercalating dye, YOYO-1 is known to deform, unwind, and often break double-stranded DNA molecules when induced by photons.[245,246] Thus, as shown in Fig. 10c, YOYO-1 stained DNA confined in a 400 nm nanoslit broke within 10 seconds of laser illumination. However, FP-fused DNA binding protein can obviate this issue since the fluorophore in FP does not directly interact with DNA backbones. FP-DBPs do not cause photo-induced DNA cleavage or structural deformation. Thus, FP-DBP stained DNA did not break with a long exposure of up to 5 min. Instead, the DNA images disappeared due to FP bleaching.

Moreover, it is possible to overcome bleaching by reversibly staining DNA through shifting pH or adjusting salt concentration. Fig. 9d demonstrates de-staining with a pH 11 buffer and re-staining with fresh FP-DBP in a pH 8 buffer using a surface-tethered DNA molecule, which is difficult with synthetic chemicals such as YOYO-1. In particular, FP-DBP staining is compatible with surface tethering because it is responsive to changing buffers and other environments as well as the type of FP-DBP.

Fig. 11 demonstrates A/T-specific DNA staining FP-DBPs, which were recently developed to analyse sequence infor-

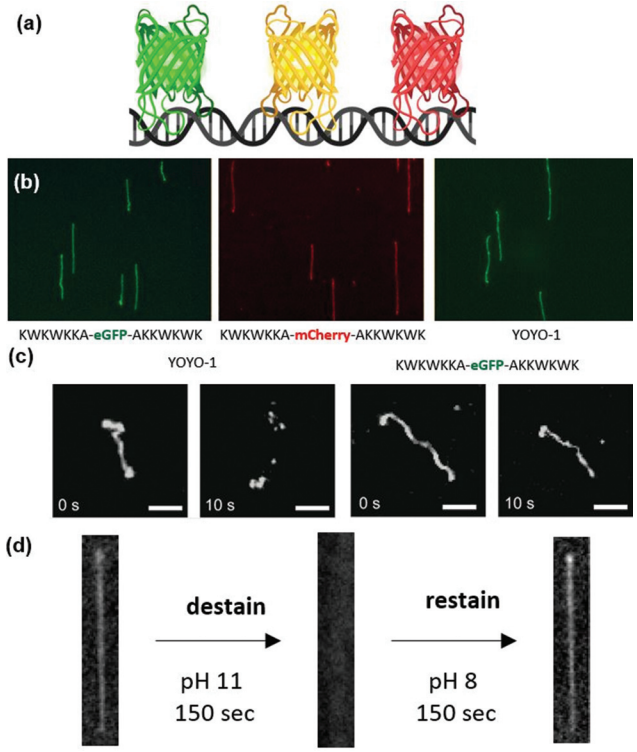

Fig. 10 FP-DBP visualisation of individual large DNA molecules. (a) Schematic of FP-DBP staining DNA (made in ©BioRender – biorender.com) (b) eGFP-DBP, mCherry-DBP, and YOYO-1 stained λ DNA (c) comparison of photolysis of YOYO-1 stained and FP-DBP stained T4 DNA (166 kb) in a 40 nm nanoslit. Scale bar = 5 μm. (d) Reversible staining capability of FP-DBP: destain with pH 11 buffer solution and restain at pH 8 1× TE buffer with FP-DBP. Reproduced from ref. 34 with permission from Oxford University Press, copyright 2015 [Creative Commons Attribution License (http://creativecommons.org/licenses/by/4.0/)].

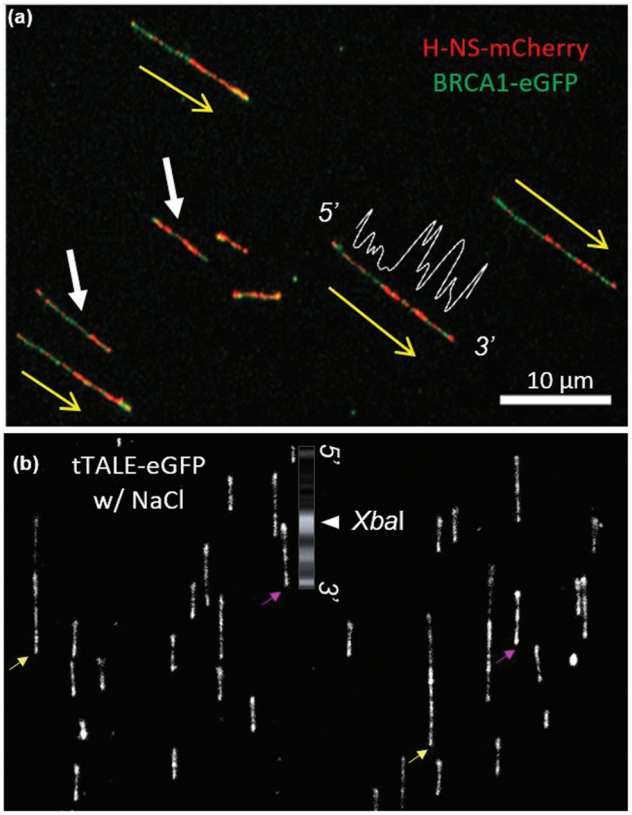

Fig. 11 A/T specific patterned λ DNA using FP-DBP (a) combination of A/T specific H-NS-mCherry and non-specific BRCA-eGFP in λ DNA Reproduced from ref. 38 from permission from The Royal Society of Chemistry, copyright 2019. (b) tethered DNA digested with *Xba*I and stained with tTALE-FP in 60 mM NaCl 1× TE buffer. Reproduced from ref. 39 from permission from Springer Nature Limited, copyright 2019 [Creative Commons Attribution 4.0 International License (http://creativecommons.org/licenses/by/4.0/)].

mation by visualising A/T-specific patterns.[38,39] As shown in Fig. 11a, H-NS-mCherry (histone-like nucleoid-structural protein) stains AT specific regions, and BRCA1-eGFP works as complementary co-staining reagents since they bind to DNA backbones homogenously. Consistent image patterns allowed the λ DNA molecules to be aligned based on three distinct red spots on a green DNA backbone. From this image, the sequence-specific patterns provide firm evidence of the molecular orientation as well as interpret a fragment in the context of the genomic map. As shown in Fig. 11b, tTALE-eGFP (truncated transcription activator-like effector) is also capable of AT-specific DNA staining.[39] Instead of labelling the target sequence of TGTCTGT, tTALE-eGFP has an A/T specific binding pattern at 40 to 100 mM NaCl concentrations. This feature allows DNA molecules to be monitored during biochemical reactions and using another stain to watch the result of the reaction with an appropriate NaCl concentration. Fig. 10b is an example of restriction enzyme (*Xba*I) digested λ DNA, which was stained with tTALE-FP and 60 mM NaCl added to 1× TE buffer. This image allows us to confirm the digestion sites in a DNA physical map. Sequence-specific FP-DBP staining makes it possible to observe genome-specific patterns reflecting the distribution of A/T rich regions. Consequently, two-colour FP-DBPs and tTALE-FP produce a sequence-specific DNA physical map for efficient optical identification of single DNA molecules.

Future perspectives

The development of fluorescence microscopy enables the observation of previously invisible cellular mechanisms. Many kinds of FP-DBPs have been developed to visualise DNA molecules both in cells and single-molecule platforms, allowing the study of DNA-related cellular mechanisms such as protein–DNA interaction, chromosome dynamics, and DNA transcription, replication, and repair. EGFP and mCherry are popular, but there are many other FPs with better characteristics. The database website, FPbase.org, is a powerful tool to evaluate all these attributes and references when choosing an appropriate FP. Their data enable to construct a few characteristic graphs showing their brightness, photo-stability, pK_a, and maturation

time. These characteristics provide information for choosing an appropriate FP for a particular purpose. For example, mRuby3 can be useful for applying mRuby3-tagged DNA binding proteins to the study of DNA-related mechanisms, because it has high brightness, and long-bleaching time, while it has not been used for DNA binding proteins.

This review categorised FP-DBP applications in cell biology. However, it is notable that there are many DNA binding proteins that have never been used for FP-DBP. For example, the human genome has 2600 proteins containing DNA-binding domains, and the yeast genome (*S. cerevisiae*) has 300 transcription factors. Genomes from different organisms encode different sequences for related DNA-binding proteins. Thus, it is very likely that new FP-DBP can be developed by connecting these DNA-binding proteins.

So far, most studies using FP-DBP have focused on visualisation in cells. In contrast, applying FP-DBP to single DNA molecules, which is a powerful platform for the visualisation of DNA-binding proteins on a stretched DNA molecule, is a relatively new field. This platform has the capacity to monitor moving proteins and its activity on large DNA molecules. More importantly, it is fascinating to observe DNA–protein interactions in the context of a genomic map based on sequence-specific staining. Therefore, single-molecule DNA observation using FP-DBP is a powerful tool to provide detailed information such as binding sites on DNA molecules, real-time movement of proteins on the DNA backbone, and DNA staining patterns.

Conflicts of interest

There are no conflicts to declare.

Acknowledgements

This work was supported by the Nuclear R&D program and a National Research Foundation of Korea (NRF) grant [NRF-2016M3A9B6947831, NRF-2016R1A6A1A03012845, and NRF-2020R1A2B5B02001831]. We would like to thank Editage (http://www.editage.co.kr) for English language editing.

Notes and references

1 J. Lee, Y. Kim, S. Lee and K. Jo, *Electrophoresis*, 2015, **36**, 2057–2071.
2 Y. Michaeli, T. Shahal, D. Torchinsky, A. Grunwald, R. Hoch and Y. Ebenstein, *Chem. Commun.*, 2013, **49**, 8599–8601.
3 M. Levy-Sakin, A. Grunwald, S. Kim, N. R. Gassman, A. Gottfried, J. Antelman, Y. Kim, S. O. Ho, R. Samuel, X. Michalet, R. R. Lin, T. Dertinger, A. S. Kim, S. Chung, R. A. Colyer, E. Weinhold, S. Weiss and Y. Ebenstein, *ACS Nano*, 2014, **8**, 14–26.
4 J. Lee, H. S. Park, S. Lim and K. Jo, *Chem. Commun.*, 2013, **49**, 4740–4742.
5 S. Zirkin, S. Fishman, H. Sharim, Y. Michaeli, J. Don and Y. Ebenstein, *J. Am. Chem. Soc.*, 2014, **136**, 7771–7776.
6 J. Lee, Y. Kim, S. Lim and K. Jo, *Analyst*, 2016, **141**, 847–852.
7 Y. Kang, J. Lee, J. Kim, Y. Oh, D. Kim, J. Lee, S. Lim and K. Jo, *Analyst*, 2016, **141**, 4326–4331.
8 Y. Kim, Z. B. Shi, H. S. Zhang, I. J. Finkelstein and H. T. Yu, *Science*, 2019, **366**, 1345–1349.
9 S. M. Hamdan, J. J. Loparo, M. Takahashi, C. C. Richardson and A. M. van Oijen, *Nature*, 2009, **457**, 336–U339.
10 J. E. Graham, K. J. Marians and S. C. Kowalczykowski, *Cell*, 2017, **169**, 1201–1213.
11 I. J. Finkelstein, M. L. Visnapuu and E. C. Greene, *Nature*, 2010, **468**, 983–987.
12 T. Yeom, J. Lee, S. Lee, S. Kang, K. R. Kim, B. Han, H. S. Lee and K. Jo, *Analyst*, 2014, **139**, 2432–2439.
13 G. Giemsa, *Centralbl. Bakteriol., Parasitenkd. Infektionskrankh., Abt. 1*, 1904, **32**, 307–313.
14 H. V. Thorne, *Virology*, 1966, **29**, 234–239.
15 P. B. C. Aaij, *Biochim. Biophys. Acta, Nucleic Acids Protein Synth.*, 1972, **269**, 192–200.
16 W. C. Russell, C. Newman and D. H. Williamson, *Nature*, 1975, **253**, 461–462.
17 A. N. Glazer and H. S. Rye, *Nature*, 1992, **359**, 859–861.
18 H. S. Rye, S. Yue, D. E. Wemmer, M. A. Quesada, R. P. Haugland, R. A. Mathies and A. N. Glazer, *Nucleic Acids Res.*, 1992, **20**, 2803–2812.
19 R. P. Haugland, S. T. Yue, P. J. Millard and B. L. Roth, *US pat.*, 5436134, 1995.
20 P. R. Langer-Safer, M. Levine and D. C. Ward, *Proc. Natl. Acad. Sci. U. S. A.*, 1982, **79**, 4381–4385.
21 J. G. Bauman, J. Wiegant, P. Borst and P. van Duijn, *Exp. Cell Res.*, 1980, **128**, 485–490.
22 H. H. Heng, J. Squire and L. C. Tsui, *Proc. Natl. Acad. Sci. U. S. A.*, 1992, **89**, 9509–9513.
23 I. Parra and B. Windle, *Nat. Genet.*, 1993, **5**, 17–21.
24 D. C. Schwartz, X. Li, L. I. Hernandez, S. P. Ramnarain, E. J. Huff and Y. K. Wang, *Science*, 1993, **262**, 110–114.
25 A. H. Samad, W. W. Cai, X. H. Hu, B. Irvin, J. P. Jing, J. Reed, X. Meng, J. Huang, E. Huff, B. Porter, A. Shenkar, T. Anantharaman, B. Mishra, V. Clarke, E. Dimalanta, J. Edington, C. Hiort, R. Rabbah, J. Skiada and D. C. Schwartz, *Nature*, 1995, **378**, 516–517.
26 K. Jo, D. M. Dhingra, T. Odijk, J. J. de Pablo, M. D. Graham, R. Runnheim, D. Forrest and D. C. Schwartz, *Proc. Natl. Acad. Sci. U. S. A.*, 2007, **104**, 2673–2678.
27 M. Xiao, A. Phong, C. Ha, T. F. Chan, D. M. Cai, L. Leung, E. Wan, A. L. Kistler, J. L. DeRisi, P. R. Selvin and P. Y. Kwok, *Nucleic Acids Res.*, 2007, **35**, e16.
28 K. L. Kounovsky-Shafer, J. P. Hernandez-Ortiz, K. Potamousis, G. Tsvid, M. Place, P. Ravindran, K. Jo,

S. Zhou, T. Odijk, J. J. de Pablo and D. C. Schwartz, *Proc. Natl. Acad. Sci. U. S. A.*, 2017, **114**, 13400–13405.
29 C. Vranken, J. Deen, L. Dirix, T. Stakenborg, W. Dehaen, V. Leen, J. Hofkens and R. K. Neely, *Nucleic Acids Res.*, 2014, **42**, e50.
30 R. K. Neely, P. Dedecker, J. I. Hotta, G. Urbanaviciute, S. Klimasauskas and J. Hofkens, *Chem. Sci.*, 2010, **1**, 453–460.
31 W. Reisner, N. B. Larsen, A. Silahtaroglu, A. Kristensen, N. Tommerup, J. O. Tegenfeldt and H. Flyvbjerg, *Proc. Natl. Acad. Sci. U. S. A.*, 2010, **107**, 13294–13299.
32 L. K. Nyberg, F. Persson, J. Berg, J. Bergstrom, E. Fransson, L. Olsson, M. Persson, A. Stalnacke, J. Wigenius, J. O. Tegenfeldt and F. Westerlund, *Biochem. Biophys. Res. Commun.*, 2012, **417**, 404–408.
33 S. Lee, Y. Kawamoto, T. Vaijayanthi, J. Park, J. Bae, J. Kim-Ha, H. Sugiyama and K. Jo, *Nucleic Acids Res.*, 2018, **46**, e108.
34 S. Lee, Y. Oh, J. Lee, S. Choe, S. Lim, H. S. Lee, K. Jo and D. C. Schwartz, *Nucleic Acids Res.*, 2016, **44**, e6.
35 K. I. Kim, S. Lee, X. Jin, S. J. Kim, K. Jo and J. H. Lee, *Small*, 2017, **13**, 1601926.
36 S. Lee, C. Wang, J. Song, D. G. Kim, Y. Oh, W. Ko, J. Lee, J. Park, H. S. Lee and K. Jo, *RSC Adv.*, 2016, **6**, 46291–46298.
37 K. I. Kim, S. Yoon, J. Chang, S. Lee, H. H. Cho, S. H. Jeong, K. Jo and J. H. Lee, *Small*, 2020, e1905821, DOI: 10.1002/smll.201905821.
38 J. Park, S. Lee, N. Won, E. Shin, S. H. Kim, M. Y. Chun, J. Gu, G. Y. Jung, K. I. Lim and K. Jo, *Analyst*, 2019, **144**, 921–927.
39 E. Shin, W. Kim, S. Lee, J. Bae, S. Kim, W. Ko, H. S. Seo, S. Lim, H. S. Lee and K. Jo, *Sci. Rep.*, 2019, **9**, 17197.
40 T. Sekiguchi, Y. Nohiro, Y. Nakamura, N. Hisamoto and T. Nishimoto, *Mol. Cell. Biol.*, 1991, **11**, 3317–3325.
41 G. W. Fang and T. R. Cech, *J. Cell Biol.*, 1995, **130**, 243–253.
42 R. Saha, U. Banik, S. Bandopadhyay, N. C. Mandal, B. Bhattacharyya and S. Roy, *J. Biol. Chem.*, 1992, **267**, 5862–5867.
43 G. J. Latham, P. Pietroni, F. Dong, M. C. Young and P. H. vonHippel, *J. Mol. Biol.*, 1996, **264**, 426–439.
44 A. Granéli, C. C. Yeykal, R. B. Robertson and E. C. Greene, *Proc. Natl. Acad. Sci. U. S. A.*, 2006, **103**, 1221–1226.
45 M. Chalfie, Y. Tu, G. Euskirchen, W. W. Ward and D. C. Prasher, *Science*, 1994, **263**, 802–805.
46 B. N. G. Giepmans, S. R. Adams, M. H. Ellisman and R. Y. Tsien, *Science*, 2006, **312**, 217–224.
47 T. J. Lambert, *Nat. Methods*, 2019, **16**, 277–278.
48 I. I. Shemiakina, G. V. Ermakova, P. J. Cranfill, M. A. Baird, R. A. Evans, E. A. Souslova, D. B. Staroverov, A. Y. Gorokhovatsky, E. V. Putintseva, T. V. Gorodnicheva, T. V. Chepurnykh, L. Strukova, S. Lukyanov, A. G. Zaraisky, M. W. Davidson, D. M. Chudakov and D. Shcherbo, *Nat. Commun.*, 2012, **3**, 1204.
49 Y. Shen, Y. C. Chen, J. G. Wu, N. C. Shaner and R. E. Campbell, *PLoS One*, 2017, **12**, e0171257.
50 S. Saeidnia and M. Abdollahi, *Daru*, 2013, **21**, 71.
51 V. L. Singer, T. E. Lawlor and S. Yue, *Mutat. Res.*, 1999, **439**, 37–47.
52 M. A. Tycon, C. F. Dial, K. Faison, W. Melvin and C. J. Fecko, *Anal. Biochem.*, 2012, **426**, 13–21.
53 A. S. Biebricher, I. Heller, R. F. H. Roijmans, T. P. Hoekstra, E. J. G. Peterman and G. J. L. Wuite, *Nat. Commun.*, 2015, **6**, 7304.
54 E. Snapp, *Curr. Protoc. Cell Biol.*, 2005, **27**, 21.4.1–21.4.13.
55 Addgene, *FLUORESCENT PROTEINS 101*, 2017.
56 A. Miyawaki, A. Sawano and T. Kogure, *Nat. Cell Biol.*, 2003, S1–S7.
57 M. Ormo, A. B. Cubitt, K. Kallio, L. A. Gross, R. Y. Tsien and S. J. Remington, *Science*, 1996, **273**, 1392–1395.
58 T. N. Campbell and F. Y. M. Choy, *Mol. Biol. Today*, 2001, **2**, 1–4.
59 M. Tanudji, S. Hevi and S. L. Chuck, *J. Cell Sci.*, 2002, **115**, 3849–3857.
60 T. D. Craggs, *Chem. Soc. Rev.*, 2009, **38**, 2865–2875.
61 X. Y. Chen, J. L. Zaro and W. C. Shen, *Adv. Drug Delivery Rev.*, 2013, **65**, 1357–1369.
62 M. Ratz, I. Testa, S. W. Hell and S. Jakobs, *Sci. Rep.*, 2015, **5**, 9592.
63 E. Palmer and T. Freeman, *Comp. Funct. Genomics*, 2004, **5**, 342–353.
64 E. M. Merzlyak, J. Goedhart, D. Shcherbo, M. E. Bulina, A. S. Shcheglov, A. F. Fradkov, A. Gaintzeva, K. A. Lukyanov, S. Lukyanov, T. W. J. Gadella and D. M. Chudakov, *Nat. Methods*, 2007, **4**, 555–557.
65 L. Wang, W. C. Jackson, P. A. Steinbach and R. Y. Tsien, *Proc. Natl. Acad. Sci. U. S. A.*, 2004, **101**, 16745–16749.
66 L. Wang and R. Y. Tsien, *Nat. Protoc.*, 2006, **1**, 1346–1350.
67 G. G. Lambert, H. Depernet, G. Gotthard, D. T. Schultz, I. Navizet, T. Lambert, D. S. Bindels, V. Levesque, J. N. Moffatt, A. Salih, A. Royant and N. C. Shaner, *bioRxiv*, 2019, 677344, DOI: 10.1101/677344.
68 M. D. Wiens, Y. Shen, X. Li, M. A. Salem, N. Smisdom, W. Zhang, A. Brown and R. E. Campbell, *ChemBioChem*, 2016, **17**, 2361–2367.
69 H. Y. Ren, B. Yang, C. Ma, Y. S. Hu, P. G. Wang and L. Wane, *ACS Chem. Biol.*, 2016, **11**, 2679–2684.
70 J. Chu, R. D. Haynes, S. Y. Corbel, P. P. Li, E. Gonzalez-Gonzalez, J. S. Burg, N. J. Ataie, A. J. Lam, P. J. Cranfill, M. A. Baird, M. W. Davidson, H. L. Ng, K. C. Garcia, C. H. Contag, K. Shen, H. M. Blau and M. Z. Lin, *Nat. Methods*, 2014, **11**, 572–578.
71 D. Shcherbo, E. M. Merzlyak, T. V. Chepurnykh, A. F. Fradkov, G. V. Ermakova, E. A. Solovieva, K. A. Lukyanov, E. A. Bogdanova, A. G. Zaraisky, S. Lukyanov and D. M. Chudakov, *Nat. Methods*, 2007, **4**, 741–746.
72 N. C. Shaner, M. Z. Lin, M. R. McKeown, P. A. Steinbach, K. L. Hazelwood, M. W. Davidson and R. Y. Tsien, *Nat. Methods*, 2008, **5**, 545–551.

73 B. T. Bajar, E. S. Wang, A. J. Lam, B. B. Kim, C. L. Jacobs, E. S. Howe, M. W. Davidson, M. Z. Lin and J. Chu, *Sci. Rep.*, 2016, **6**, 20889.
74 D. S. Bindels, L. Haarbosch, L. van Weeren, M. Postma, K. E. Wieser, M. Mastop, S. Aumonier, G. Gotthard, A. Royant, M. A. Hink and T. W. J. Gadella, *Nat. Methods*, 2017, **14**, 53–56.
75 B. T. Bajar, A. J. Lam, R. K. Badiee, Y. H. Oh, J. Chu, X. X. Zhou, N. Kim, B. B. Kim, M. Y. Chung, A. L. Yablonovitch, B. F. Cruz, K. Kulalert, J. J. Tao, T. Meyer, X. D. Su and M. Z. Lin, *Nat. Methods*, 2016, **13**, 993–996.
76 M. Z. Lin, M. R. McKeown, H. L. Ng, T. A. Aguilera, N. C. Shaner, R. E. Campbell, S. R. Adams, L. A. Gross, W. Ma, T. Alber and R. Y. Tsien, *Chem. Biol.*, 2009, **16**, 1169–1179.
77 N. C. Shaner, G. G. Lambert, A. Chammas, Y. H. Ni, P. J. Cranfill, M. A. Baird, B. R. Sell, J. R. Allen, R. N. Day, M. Israelsson, M. W. Davidson and J. Wang, *Nat. Methods*, 2013, **10**, 407–409.
78 H. W. Ai, J. N. Henderson, S. J. Remington and R. E. Campbell, *Biochem. J.*, 2006, **400**, 531–540.
79 H. W. Ai, S. G. Olenych, P. Wong, M. W. Davidson and R. E. Campbell, *BMC Biol.*, 2008, **6**, 13.
80 J. Goedhart, D. von Stetten, M. Noirclerc-Savoye, M. Lelimousin, L. Joosen, M. A. Hink, L. van Weeren, T. W. J. Gadella and A. Royant, *Nat. Commun.*, 2012, **3**, 751.
81 H. Shinoda, Y. Q. Ma, R. Nakashima, K. Sakurai, T. Matsuda and T. Nagai, *Cell Chem. Biol.*, 2018, **25**, 330–338.
82 N. C. Shaner, R. E. Campbell, P. A. Steinbach, B. N. G. Giepmans, A. E. Palmer and R. Y. Tsien, *Nat. Biotechnol.*, 2004, **22**, 1567–1572.
83 O. M. Subach, P. J. Cranfill, M. W. Davidson and V. V. Verkhusha, *PLoS One*, 2011, **6**, e28674.
84 E. Spiess, F. Bestvater, A. Heckel-Pompey, K. Toth, M. Hacker, G. Stobrawa, T. Feurer, C. Wotzlaw, U. Berchner-Pfannschmidt, T. Porwol and H. Acker, *J. Microsc.*, 2005, **217**, 200–204.
85 G. J. Kremers, J. Goedhart, E. B. van Munster and T. W. J. Gadella, *Biochemistry*, 2006, **45**, 6570–6580.
86 O. Griesbeck, G. S. Baird, R. E. Campbell, D. A. Zacharias and R. Y. Tsien, *J. Biol. Chem.*, 2001, **276**, 29188–29194.
87 T. Nagai, K. Ibata, E. S. Park, M. Kubota, K. Mikoshiba and A. Miyawaki, *Nat. Biotechnol.*, 2002, **20**, 87–90.
88 S. Gurrieri, S. B. Smith, K. S. Wells, I. D. Johnson and C. Bustamante, *Nucleic Acids Res.*, 1996, **24**, 4759–4767.
89 G. T. Dempsey, J. C. Vaughan, K. H. Chen, M. Bates and X. Zhuang, *Nat. Methods*, 2011, **8**, 1027–1036.
90 J. H. M. van der Velde, J. Oelerich, J. Huang, J. H. Smit, A. A. Jazi, S. Galiani, K. Kolmakov, G. Guoridis, C. Eggeling, A. Herrmann, G. Roelfes and T. Cordes, *Nat. Commun.*, 2016, **7**, 10144.
91 J. Icha, M. Weber, J. C. Waters and C. Norden, *Bioessays*, 2017, **39**, 1700003.
92 J. Wiedenmann, F. Oswald and G. U. Nienhaus, *IUBMB Life*, 2009, **61**, 1029–1042.
93 L. Hostettler, L. Grundy, S. Kaser-Pebernard, C. Wicky, W. R. Schafer and D. A. Glauser, *G3-Genes Genom Genet*, 2017, **7**, 607–615.
94 E. A. Rodriguez, R. E. Campbell, J. Y. Lin, M. Z. Lin, A. Miyawaki, A. E. Palmer, X. K. Shu, J. Zhang and R. Y. Tsien, *Trends Biochem. Sci.*, 2017, **42**, 111–129.
95 M. D. Leonetti, S. Sekine, D. Kamiyama, J. S. Weissman and B. Huang, *Proc. Natl. Acad. Sci. U. S. A.*, 2016, **113**, E3501–E3508.
96 S. Zhong, F. Rivera-Molina, A. Rivetta, D. Toomre, J. Santos-Sacchi and D. Navaratnam, *J. Neurosci. Methods*, 2019, **313**, 68–76.
97 D. K. Tiwari, Y. Arai, M. Yamanaka, T. Matsuda, M. Agetsuma, M. Nakano, K. Fujita and T. Nagai, *Nat. Methods*, 2015, **12**, 515–518.
98 S. Karasawa, T. Araki, T. Nagai, H. Mizuno and A. Miyawaki, *Biochem. J.*, 2004, **381**, 307–312.
99 D. Shcherbo, C. S. Murphy, G. V. Ermakova, E. A. Solovieva, T. V. Chepurnykh, A. S. Shcheglov, V. V. Verkhusha, V. Z. Pletnev, K. L. Hazelwood, P. M. Roche, S. Lukyanov, A. G. Zaraisky, M. W. Davidson and D. M. Chudakov, *Biochem. J.*, 2009, **418**, 567–574.
100 H. W. Ai, N. C. Shaner, Z. H. Cheng, R. Y. Tsien and R. E. Campbell, *Biochemistry*, 2007, **46**, 5904–5910.
101 F. V. Subach, O. M. Subach, I. S. Gundorov, K. S. Morozova, K. D. Piatkevich, A. M. Cuervo and V. V. Verkhusha, *Nat. Chem. Biol.*, 2009, **5**, 118–126.
102 O. M. Subach, I. S. Gundorov, M. Yoshimura, F. V. Subach, J. H. Zhang, D. Gruenwald, E. A. Souslova, D. M. Chudakov and V. V. Verkhusha, *Chem. Biol.*, 2008, **15**, 1116–1124.
103 A. Khmelinskii, P. J. Keller, A. Bartosik, M. Meurer, J. D. Barry, B. R. Mardin, A. Kaufmann, S. Trautmann, M. Wachsmuth, G. Pereira, W. Huber, E. Schiebel and M. Knop, *Nat. Biotechnol.*, 2012, **30**, 708–714.
104 E. Balleza, J. M. Kim and P. Cluzel, *Nat. Methods*, 2018, **15**, 47–51.
105 H. W. Ai, K. L. Hazelwood, M. W. Davidson and R. E. Campbell, *Nat. Methods*, 2008, **5**, 401–403.
106 L. M. Costantini, M. Baloban, M. L. Markwardt, M. Rizzo, F. Guo, V. V. Verkhusha and E. L. Snapp, *Nat. Commun.*, 2015, **6**, 7670.
107 V. Fernandez-Luna, P. B. Coto and R. D. Costa, *Angew. Chem., Int. Ed.*, 2018, **57**, 8826–8836.
108 N. Aliye, A. Fabbretti, G. Lupidi, T. Tsekoa and R. Spurio, *Appl Microbiol Biot*, 2015, **99**, 1205–1216.
109 Y. Ravikumar, S. P. Nadarajan, C. S. Lee, J. K. Rhee and H. Yun, *J. Microbiol. Biotechnol.*, 2015, **25**, 503–510.
110 F. Steiert, E. P. Petrov, P. Schultz, P. Schwille and T. Weidemann, *Biophys. J.*, 2018, **114**, 2419–2431.
111 H. Katayama, A. Yamamoto, N. Mizushima, T. Yoshimori and A. Miyawaki, *Cell Struct. Funct.*, 2008, **33**, 1–12.
112 J. R. Houser, E. Ford, S. M. Chatterjea, S. Maleri, T. C. Elston and B. Errede, *Yeast*, 2012, **29**, 519–530.

113 N. Alonso, R. Guillen, J. W. Chambers and F. Leng, *Nucleic Acids Res.*, 2015, **43**, e52.
114 P. L. Kastritis and A. M. Bonvin, *J. R. Soc., Interface*, 2013, **10**, 20120835.
115 K. P. Williams, X. H. Liu, T. N. M. Schumacher, H. Y. Lin, D. A. Ausiello, P. S. Kim and D. P. Bartel, *Proc. Natl. Acad. Sci. U. S. A.*, 1997, **94**, 11285–11290.
116 J. K. Flores, R. Kariawasam, A. X. Gimenez, S. Helder, L. Cubeddu, R. Gamsjaeger and S. F. Ataide, *Curr. Protein Pept. Sci.*, 2015, **16**, 727–734.
117 A. Friedler, D. B. Veprintsev, S. M. V. Freund, K. I. von Glos and A. R. Fersht, *Structure*, 2005, **13**, 629–636.
118 T. Brandt, M. Petrovich, A. C. Joerger and D. B. Veprintsev, *BMC Genomics*, 2009, **10**, 628.
119 T. K. Nomanbhoy and R. A. Cerione, *J. Biol. Chem.*, 1996, **271**, 10004–10009.
120 E. Fabini, B. Zambelli, L. Mazzei, S. Ciurli and C. Bertucci, *Anal. Bioanal. Chem.*, 2016, **408**, 7971–7980.
121 D. T. Dang and A. T. Phan, *ChemBioChem*, 2016, **17**, 42–45.
122 T. P. P. Tuom, T. T. Truong, L. T.T Le, D. H. Nguyen, H. D. Nguyen and D. T. Dang, *Sci. Technol. Develop. J.*, 2018, **21**, 84–89.
123 C. Dornblut, N. Quinn, S. Monajambashi, L. Prendergast, C. van Vuuren, S. Munch, W. Deng, H. Leonhardt, M. C. Cardoso, C. Hoischen, S. Diekmann and K. F. Sullivan, *Open Biol.*, 2014, **4**, 130229.
124 J. Lawrimore, K. S. Bloom and E. D. Salmon, *J. Cell Biol.*, 2011, **195**, 573–582.
125 S. Orthaus, C. Biskup, B. Hoffmann, C. Hoischen, S. Ohndorf, K. Benndorf and S. Diekmann, *ChemBioChem*, 2008, **9**, 77–92.
126 R. D. Shelby, K. M. Hahn and K. F. Sullivan, *J. Cell Biol.*, 1996, **135**, 545–557.
127 K. Lisaingo, E. J. Uringa and P. M. Lansdorp, *Mol. Biol. Cell*, 2014, **25**, 1958–1968.
128 K. Schenk, A. B. Hervas, T. C. Roesch, M. Eisemann, B. A. Schmitt, S. Dahlke, L. Kleine-Borgmann, S. M. Murray and P. L. Graumann, *PLoS Genet.*, 2017, **13**, e1006561.
129 J. Majka, J. Zakrzewska-Czerwinska and W. Messer, *J. Biol. Chem.*, 2001, **276**, 6243–6252.
130 J. T. Mika, A. Vanhecke, P. Dedecker, T. Swings, J. Vangindertael, B. Van den Bergh, J. Michiels and J. Hofkens, *Faraday Discuss.*, 2015, **184**, 425–450.
131 M. Dafny-Yelin, A. Levy, R. Dafny and T. Tzfira, *Plant Physiol.*, 2015, **167**, 153–163.
132 L. Marchetti, L. Comelli, B. D'Innocenzo, L. Puzzi, S. Luin, D. Arosio, M. Calvello, R. Mendoza-Maldonado, F. Peverali, F. Trovato, S. Riva, G. Biamonti, G. Abdurashidova, F. Beltram and A. Falaschi, *Nucleic Acids Res.*, 2010, **38**, 8105–8119.
133 L. Comelli, L. Marchetti, D. Arosio, S. Riva, G. Abdurashidova, F. Beltram and A. Falaschi, *Cell Cycle*, 2009, **8**, 454–459.
134 W. M. Knosp, C. Saneyoshi, S. M. Shou, H. P. Bachinger and H. S. Stadler, *J. Biol. Chem.*, 2007, **282**, 6843–6853.
135 W. Y. Lv, J. J. Wu, Z. Xu, H. Dai, Z. H. Ma and Z. Y. Wang, *Curr. Genet.*, 2019, **65**, 981–994.
136 Y. Wang, P. J. Hu, H. H. Li, Y. L. Wang, L. K. Long, K. Li, X. L. Zhang, Y. Y. Pan and G. Liu, *Fungal Genet Biol*, 2018, **118**, 1–9.
137 T. Gross, S. Broholm and A. Becker, *Front. Plant Sci.*, 2018, **9**, 835.
138 X. L. Zhang, Y. Liu, X. Z. Wang, X. Y. Sun, C. Y. Zhang and S. G. Zheng, *PLoS One*, 2017, **12**, e0181653.
139 M. Tsutsumi, H. Muto, S. Myoba, M. Kimoto, A. Kitamura, M. Kamiya, T. Kikukawa, S. Takiya, M. Demura, K. Kawano, M. Kinjo and T. Aizawa, *FEBS Open Bio*, 2016, **6**, 106–125.
140 S. E. Taylor, J. Bagnall, D. Mason, R. Levy, D. G. Fernig and V. See, *Open Biol.*, 2016, **6**, 160195.
141 M. S. Chung, S. Lee, J. H. Min, P. Huang, H. W. Ju and C. S. Kim, *Plant Physiol. Biochem.*, 2016, **104**, 155–164.
142 D. K. Papadopoulos, A. J. Krmpot, S. N. Nikolic, R. Krautz, L. Terenius, P. Tomancak, R. Rigler, W. J. Gehring and V. Vukojevic, *Mech. Dev.*, 2015, **138**, 218–225.
143 F. Cornille, P. Emery, W. Schuler, C. Lenoir, B. Mach, B. P. Rogues and W. Reith, *Nucleic Acids Res.*, 1998, **26**, 2143–2149.
144 K. Min, H. Son, J. Y. Lim, G. J. Choi, J. C. Kim, S. D. Harris and Y. W. Lee, *Eukaryotic Cell*, 2014, **13**, 427–436.
145 P. Hortschansky, E. Ando, K. Tuppatsch, H. Arikawa, T. Kobayashi, M. Kato, H. Haas and A. A. Brakhage, *J. Biol. Chem.*, 2015, **290**, 6058–6070.
146 F. Gsaller, P. Hortschansky, S. R. Beattie, V. Klammer, K. Tuppatsch, B. E. Lechner, N. Rietzschel, E. R. Werner, A. A. Vogan, D. Chung, U. Muhlenhoff, M. Kato, R. A. Cramer, A. A. Brakhage and H. Haas, *EMBO J.*, 2014, **33**, 2261–2276.
147 D. Tsugama, S. K. Liu and T. Takano, *Plant Physiol.*, 2012, **159**, 144–155.
148 S. Chatterjee, Y. N. Zhou, S. Roy and S. Adhya, *Proc. Natl. Acad. Sci. U. S. A.*, 1997, **94**, 2957–2962.
149 Z. Qian, E. K. Dimitriadis, R. Edgar, P. Eswaramoorthy and S. Adhya, *Proc. Natl. Acad. Sci. U. S. A.*, 2012, **109**, 11336–11341.
150 C. S. Lam, T. K. Mistri, Y. H. Foo, T. Sudhaharan, H. T. Gan, D. Rodda, L. H. Lim, C. Chou, P. Robson, T. Wohland and S. Ahmed, *Biochem. J.*, 2012, **448**, 21–33.
151 T. K. Mistri, W. Arindrarto, W. P. Ng, C. Y. Wang, L. H. Lim, L. L. Sun, I. Chambers, T. Wohland and P. Robson, *Biochem. J.*, 2018, **475**, 1075–1089.
152 X. Zhang, H. W. Ju, M. S. Chung, P. Huang, S. J. Ahn and C. S. Kim, *Plant Cell Physiol.*, 2011, **52**, 138–148.
153 C. Perez-Borrajero, M. Okon and L. P. McIntosh, *J. Mol. Biol.*, 2016, **428**, 2372–2391.
154 J. J. Qiu, H. Chu, X. Lu, X. Jiang and S. Dong, *Oncogene*, 2011, **30**, 967–977.
155 C. Chen and R. Bundschuh, *Nucleic Acids Res.*, 2014, **42**, 9753–9760.

156 P. Oliveira and P. Lindblad, *J. Bacteriol.*, 2011, **193**, 3804–3814.
157 F. J. Jin, T. Takahashi, K. Matsushima, S. Hara, Y. Shinohara, J. Maruyama, K. Kitamoto and Y. Koyama, *Eukaryotic Cell*, 2011, **10**, 945–955.
158 R. Lall, S. Kuruvilla and K. Prufer, *Cell Biol. Int.*, 2009, **33**, 447–452.
159 M. Jbel, A. Mercier, B. Pelletier, J. Beaudoin and S. Labbe, *Eukaryotic Cell*, 2009, **8**, 649–664.
160 Y. Zhang, G. Zhang, N. Xia, X. J. Wang, L. L. Huang and Z. S. Kang, *Physiol. Plant Pathol.*, 2008, **73**, 88–94.
161 A. Spielvogel, H. Findon, H. N. Arst, L. Araujo-Bazan, P. Hernandez-Ortiz, U. Stahl, V. Meyer and E. A. Espeso, *Biochem. J.*, 2008, **414**, 419–429.
162 M. Panda, D. F. Jiang and H. W. Jarrett, *J. Chromatogr. A*, 2008, **1202**, 75–82.
163 J. Lee, J. J. Park, S. L. Kim, J. Yim and G. An, *Plant Mol. Biol.*, 2007, **65**, 487–499.
164 T. Chuio, R. Takai, C. Akimoto-Tomiyama, S. Ando, E. Minami, Y. Nagamura, H. Kaku, N. Shibuya, M. Yasuda, H. Nakashita, K. Umemura, A. Okada, K. Okada, H. Nojiri and H. Yamane, *Biochim. Biophys. Acta, Gene Struct. Expression*, 2007, **1769**, 497–505.
165 J. Z. Yan, L. S. Xu, G. Crawford, Z. F. Wang and S. M. Burgess, *Mol. Cell. Biol.*, 2006, **26**, 155–168.
166 M. S. Stitt, K. J. Wasserloos, X. Tang, X. Liu, B. R. Pitt and C. M. St Croix, *Vasc. Pharmacol.*, 2006, **44**, 149–155.
167 H. Nakagama, G. Heinrich, J. Pelletier and D. E. Housman, *Mol. Cell. Biol.*, 1995, **15**, 1489–1498.
168 J. R. Dutton, D. Lahiri and A. Ward, *Cell Proliferation*, 2006, **39**, 519–535.
169 H. L. Zhong, A. Takeda, R. Nazari, H. Shio, G. Blobel and N. R. Yaseen, *J. Biol. Chem.*, 2005, **280**, 10675–10682.
170 H. Yamasaki, T. Sekimoto, T. Ohkubo, T. Douchi, Y. Nagata, M. Ozawa and Y. Yoneda, *Genes Cells*, 2005, **10**, 455–464.
171 T. Nagamine, Y. Kawasaki, T. Iizuka and S. Matsumoto, *J. Virol.*, 2005, **79**, 39–46.
172 X. H. Zhang, L. X. Gan, H. Y. Pan, S. D. Guo, X. W. He, S. T. Olson, A. Mesecar, S. Adam and T. G. Unterman, *J. Biol. Chem.*, 2002, **277**, 45276–45284.
173 X. S. Zhao, L. X. Gan, H. Y. Pan, D. H. Kan, M. Majeski, S. A. Adam and T. G. Unterman, *Biochem. J.*, 2004, **378**, 839–849.
174 Z. D. Sharp, D. L. Stenoien, M. G. Mancini, I. I. Ouspenski and M. A. Mancini, *J. Cell. Biochem.*, 2004, **92**, 664–678.
175 M. G. Romanelli, L. Tato', P. Lorenzi and C. Morandi, *Biochim. Biophys. Acta, Mol. Cell Res.*, 2003, **1643**, 55–64.
176 J. Fernandez-Martinez, C. V. Brown, E. Diez, J. Tilburn, H. N. Arst, M. A. Penalva and E. A. Espeso, *J. Mol. Biol.*, 2003, **334**, 667–684.
177 K. Kinoshita, Y. Kikuchi, Y. Sasakura, M. Suzuki, Y. Fujii-Kuriyama and K. Sogawa, *Nucleic Acids Res.*, 2004, **32**, 3169–3179.
178 M. Tojo, K. Matsuzaki, T. Minami, Y. Honda, H. Yasuda, T. Chiba, H. Saya, Y. Fujii-Kuriyama and M. Nakao, *J. Biol. Chem.*, 2002, **277**, 46576–46585.
179 L. X. Zhang, Z. C. Hua, J. G. Ren and A. M. Meng, *FEBS Lett.*, 2001, **503**, 25–29.
180 J. Wong, M. Funes-Duran, J. Ahlberg, J. Round, R. O'Connell, R. Miller, E. Chen, P. A. Richmond and C. A. Vierra, *DNA Cell Biol.*, 2001, **20**, 465–471.
181 M. Matsumoto, K. Hisatake, Y. Nogi and M. Tsujimoto, *J. Biol. Chem.*, 2001, **276**, 33086–33092.
182 M. Tiwari, S. Mikuni, H. Muto and M. Kinjo, *Biochem. Biophys. Res. Commun.*, 2013, **436**, 430–435.
183 J. A. Schmid, A. Birbach, R. Hofer-Warbinek, M. Pengg, U. Burner, P. G. Furtmuller, B. R. Binder and R. de Martin, *J. Biol. Chem.*, 2000, **275**, 17035–17042.
184 L. S. He, J. H. Liu, I. Collins, S. Sanford, B. O'Connell, C. J. Benham and D. Levens, *EMBO J.*, 2000, **19**, 1034–1044.
185 L. S. He, A. Weber and D. Levens, *Nucleic Acids Res.*, 2000, **28**, 4558–4565.
186 B. Hessabi, P. Ziegler, I. Schmidt, C. Hessabi and R. Walther, *Eur. J. Biochem.*, 1999, **263**, 170–177.
187 J. Herrington, L. Y. Rui, G. Y. Luo, L. Y. Yu-Lee and C. Carter-Su, *J. Biol. Chem.*, 1999, **274**, 5138–5145.
188 F. Schaper, S. Kirchhoff, G. Posern, M. Koster, A. Oumard, R. Sharf, B. Z. Levi and H. Hauser, *Biochem. J.*, 1998, **335**, 147–157.
189 K. Giese, J. Pagel and R. Grosschedl, *Proc. Natl. Acad. Sci. U. S. A.*, 1997, **94**, 12845–12850.
190 M. G. Prieve, K. L. Guttridge, J. Munguia and M. L. Waterman, *Mol. Cell. Biol.*, 1998, **18**, 4819–4832.
191 S. F. Tolic-Norrelykke, M. B. Rasmussen, F. S. Pavone, K. Berg-Sorensen and L. B. Oddershede, *Biophys. J.*, 2006, **90**, 3694–3703.
192 G. H. Patterson, S. C. Schroeder, Y. Bai, P. A. Weil and D. W. Piston, *Yeast*, 1998, **14**, 813–825.
193 M. Spirek, J. Mlcouskova, O. Belan, M. Gyimesi, G. M. Harami, E. Molnar, J. Novacek, M. Kovacs and L. Krejci, *Nucleic Acids Res.*, 2018, **46**, 3967–3980.
194 M. Saotome, K. Saito, T. Yasuda, H. Ohtomo, S. Sugiyama, Y. Nishimura, H. Kurumizaka and W. Kagawa, *iScience*, 2018, **3**, 50–62.
195 D. P. Waterman, F. Zhou, K. Li, C. S. Lee, M. Tsabar, V. V. Eapen, A. Mazzella and J. E. Haber, *PLoS Genet.*, 2019, **15**, e1008001.
196 D. V. Gataulin, J. N. Carey, J. Y. Li, P. Shah, J. T. Grubb and D. K. Bishop, *Nucleic Acids Res.*, 2018, **46**, 9510–9523.
197 H. Ghodke, B. P. Paudel, J. S. Lewis, S. Jergic, K. Gopal, Z. J. Romero, E. A. Wood, R. Woodgate, M. M. Cox and A. M. van Oijen, *eLife*, 2019, **8**, e42761.
198 M. V. Kotlajich, J. Xia, Y. Zhai, H. Y. Lin, C. C. Bradley, X. Shen, Q. Mei, A. Z. Wang, E. J. Lynn, C. Shee, L. T. Chen, L. Li, K. M. Miller, C. Herman, P. J. Hastings and S. M. Rosenberg, *DNA Repair*, 2018, **72**, 86–92.
199 N. S. Moreno, J. Liu, K. M. Haas, L. L. Parker, C. Chakraborty, S. J. Kron, K. Hodges, L. D. Miller,

C. Langefeld, P. J. Robinson, S. A. Lelievre and P. A. Vidi, *Nucleic Acids Res.*, 2019, **47**, 2703–2715.
200 Y. Tome, F. Uehara, S. Miwa, S. Yano, S. Mii, E. V. Efimova, M. Bouvet, H. Kimura, H. Tsuchiya, F. Kanaya and R. M. Hoffman, *Anticancer Res.*, 2016, **36**, 3821–3826.
201 F. Uehara, S. Miwa, Y. Tome, Y. Hiroshima, S. Yano, M. Yamamoto, E. Efimova, Y. Matsumoto, H. Maehara, M. Bouvet, F. Kanaya and R. M. Hoffman, *J. Cell. Biochem.*, 2014, **115**, 1724–1728.
202 M. Koike, Y. Yutoku and A. Koike, *J. Vet. Med. Sci.*, 2014, **76**, 51–56.
203 S. M. Germann, V. Schramke, R. T. Pedersen, I. Gallina, N. Eckert-Boulet, V. H. Oestergaard and M. Lisby, *J. Cell Biol.*, 2014, **204**, 45–59.
204 C. Shee, B. D. Cox, F. Gu, E. M. Luengas, M. C. Joshi, L. Y. Chiu, D. Magnan, J. A. Halliday, R. L. Frisch, J. L. Gibson, R. B. Nehring, H. G. Do, M. Hernandez, L. Li, C. Herman, P. J. Hastings, D. Bates, R. S. Harris, K. M. Miller and S. M. Rosenberg, *eLife*, 2013, **2**, e01222.
205 M. Pediaditakis, M. Kaufenstein and P. L. Graumann, *J. Bacteriol.*, 2012, **194**, 6184–6194.
206 E. Berg, M. O. Christensen, I. D. Rosa, E. Wannagat, R. U. Janicke, L. M. Rosner, W. G. Dirks, F. Boege and C. Mielke, *DNA Repair*, 2011, **10**, 1232–1242.
207 Y. Wang, B. J. Lamarche and M. D. Tsai, *Biochemistry*, 2007, **46**, 4962–4976.
208 M. S. Luijsterburg, G. von Bornstaedt, A. M. Gourdin, A. Z. Politi, M. J. Mone, D. O. Warmerdam, J. Goedhart, W. Vermeulen, R. van Driel and T. Hofer, *J. Cell Biol.*, 2010, **189**, 445–463.
209 F. Liang, Y. Z. Guo, S. C. Hou and Q. M. Quan, *Sci. Adv.*, 2017, **3**, e1602991.
210 O. Mortusewicz, W. Roth, N. Li, M. C. Cardoso, M. Meisterernst and H. Leonhardt, *J. Cell Biol.*, 2008, **183**, 769–776.
211 S. Alekseev, M. S. Luijsterburg, A. Pines, B. Geverts, P. O. Mari, G. Giglia-Mari, H. Lans, A. B. Houtsmuller, L. H. F. Mullenders, J. H. J. Hoeijmakers and W. Vermeulen, *Mol. Cell. Biol.*, 2008, **28**, 7402–7413.
212 P. Perucca, O. Cazzalini, O. Mortusewicz, D. Necchi, M. Savio, T. Nardo, L. A. Stivala, H. Leonhardt, M. C. Cardoso and E. Prosperi, *J. Cell Sci.*, 2006, **119**, 1517–1527.
213 S. W. Liu, M. Kwon, M. Mannino, N. C. Yang, F. Renda, A. Khodjakov and D. Pellman, *Nature*, 2018, **561**, 551–555.
214 K. Ginda, I. Santi, D. Bousbaine, J. Zakrzewska-Czerwinska, D. Jakimowicz and J. McKinney, *Mol. Microbiol.*, 2017, **105**, 453–468.
215 C. Z. Zhang, A. Spektor, H. Cornils, J. M. Francis, E. K. Jackson, S. W. Liu, M. Meyerson and D. Pellman, *Nature*, 2015, **522**, 179–184.
216 P. J. Stephens, C. D. Greenman, B. Y. Fu, F. T. Yang, G. R. Bignell, L. J. Mudie, E. D. Pleasance, K. W. Lau, D. Beare, L. A. Stebbings, S. McLaren, M. L. Lin, D. J. McBride, I. Varela, S. Nik-Zainal, C. Leroy, M. M. Jia, A. Menzies, A. P. Butler, J. W. Teague, M. A. Quail, J. Burton, H. Swerdlow, N. P. Carter, L. A. Morsberger, C. Iacobuzio-Donahue, G. A. Follows, A. R. Green, A. M. Flanagan, M. R. Stratton, P. A. Futreal and P. J. Campbell, *Cell*, 2011, **144**, 27–40.
217 F. Notta, M. Chan-Seng-Yue, M. Lemire, Y. L. Li, G. W. Wilson, A. A. Connor, R. E. Denroche, S. B. Liang, A. M. K. Brown, J. C. Kim, T. Wang, J. T. Simpson, T. Beck, A. Borgida, N. Buchner, D. Chadwick, S. Hafezi-Bakhtiari, J. E. Dick, L. Heisler, M. A. Hollingsworth, E. Ibrahimov, G. H. Jang, J. Johns, L. G. T. Jorgensen, C. Law, O. Ludkovski, I. Lungu, K. Ng, D. Pasternack, G. M. Petersen, L. I. Shlush, L. Timms, M. S. Tsao, J. M. Wilson, C. K. Yung, G. Zogopoulos, J. M. S. Bartlett, L. B. Alexandrov, F. X. Real, S. P. Cleary, M. H. Roehrl, J. D. McPherson, L. D. Stein, T. J. Hudson, P. J. Campbell and S. Gallinger, *Nature*, 2016, **538**, 378–382.
218 E. H. Blackburn, *Nature*, 1991, **350**, 569–573.
219 T. de Lange, *Genes Dev.*, 2005, **19**, 2100–2110.
220 Z. Zhong, L. Shiue, S. Kaplan and T. Delange, *Mol. Cell. Biol.*, 1992, **12**, 4834–4843.
221 L. Chong, B. Vansteensel, D. Broccoli, H. Erdjumentbromage, J. Hanish, P. Tempst and T. Delange, *Science*, 1995, **270**, 1663–1667.
222 A. Bianchi, S. Smith, L. Chong, P. Elias and T. deLange, *EMBO J.*, 1997, **16**, 1785–1794.
223 J. Mierzejewska and G. Jagura-Burdzy, *Plasmid*, 2012, **67**, 1–14.
224 T. A. Leonard, P. J. Butler and J. Lowe, *EMBO J.*, 2005, **24**, 270–282.
225 T. Katayama, S. Ozaki, K. Keyamura and K. Fujimitsu, *Nat. Rev. Microbiol.*, 2010, **8**, 163–170.
226 T. T. Richardson, O. Harran and H. Murray, *Nature*, 2016, **534**, 412–488.
227 S. Slater, S. Wold, M. Lu, E. Boye, K. Skarstad and N. Kleckner, *Cell*, 1995, **82**, 927–936.
228 D. W. Russell and N. D. Zinder, *Cell*, 1987, **50**, 1071–1079.
229 M. Lu, J. L. Campbell, E. Boye and N. Kleckner, *Cell*, 1994, **77**, 413–426.
230 M. A. Martinezbalbas, A. Dey, S. K. Rabindran, K. Ozato and C. Wu, *Cell*, 1995, **83**, 29–38.
231 L. B. Schultz, N. H. Chehab, A. Malikzay and T. D. Halazonetis, *J. Cell Biol.*, 2000, **151**, 1381–1390.
232 I. Rappold, K. Iwabuchi, T. Date and J. J. Chen, *J. Cell Biol.*, 2001, **153**, 613–620.
233 J. Courcelle, A. Khodursky, B. Peter, P. O. Brown and P. C. Hanawalt, *Genetics*, 2001, **158**, 41–64.
234 N. Renzette, N. Gumlaw, J. T. Nordman, M. Krieger, S. P. Yeh, E. Long, R. Centore, R. Boonsombat and S. J. Sandler, *Mol. Microbiol.*, 2005, **57**, 1074–1085.
235 K. Misaki, S. Matsuda, T. Matsuda, T. Kusakabe and Y. Shimizu, *Chemosphere*, 2019, **235**, 169–174.

236 M. Yang, P. Jiang and R. M. Hoffman, *Anticancer Res.*, 2015, **35**, 2539–2543.
237 M. Barow, *Bioessays*, 2006, **28**, 271–281.
238 M. Wozny, M. H. Schattat, N. Mathur, K. Barton and J. Mathur, *Plant Physiol.*, 2012, **158**, 95–106.
239 C. Lungu, S. Pinter, J. Broche, P. Rathert and A. Jeltsch, *Nat. Commun.*, 2017, **8**, 649.
240 S. Bhattacharyya, M. M. Soniat, D. Walker, S. Jang, I. J. Finkelstein and R. M. Harshey, *Proc. Natl. Acad. Sci. U. S. A.*, 2018, **115**, E11614–E11622.
241 K. Jo, Y. L. Chen, J. J. de Pablo and D. C. Schwartz, *Lab Chip*, 2009, **9**, 2348–2355.
242 Y. Kim, K. S. Kim, K. L. Kounovsky, R. Chang, G. Y. Jung, J. J. dePablo, K. Jo and D. C. Schwartz, *Lab Chip*, 2011, **11**, 1721–1729.
243 S. Lee, Y. Lee, Y. Kim, C. Wang, J. Park, G. Y. Jung, Y. L. Chen, R. Chang, S. Ikeda, H. Sugiyama and K. Jo, *Polymers*, 2019, **11**, 15.
244 S. Lee and K. Jo, *JoVE*, 2016, **112**, e54141.
245 M. A. Tycon, C. F. Dial, K. Faison, W. Melvin and C. J. Fecko, *Anal. Biochem.*, 2012, **426**, 13–21.
246 C. U. Murade, V. Subramaniam, C. Otto and M. L. Bennink, *Nucleic Acids Res.*, 2010, **38**, 3423–3431.